



FFI Norwegian Defence
Research Establishment

22/02192

FFI-RAPPORT

Damper models and their impact on shock response

Øyvind Andreassen

Damper models and their impact on shock response

Øyvind Andreassen

Keywords

Sjokk
Sårbarhetsanalyse
Marinefartøy
Kjøretøy

FFI report

22/02192

Project number

1595/1594

Electronic ISBN

ISBN:978-82-464-3434-6

Approvers

Hanne Bjørk, *Research Director*
Bendik Sagsveen & Anders Helgeland, *Research Manager*

The document is electronically approved and therefore has no handwritten signature.

Copyright

© Norwegian Defence Research Establishment (FFI). The publication may be freely cited where the source is acknowledged.

Summary

Mechanical vibration and shocks may be devastating, in particular to military equipment. Therefore, vibration and shock damping are of crucial importance to military hardware. Vibrations can cause material fatigue. They can also cause emission of sound which can reveal the presence of ships and vehicles. Silence is crucial for submarine operations.

Shocks from weapons can damage equipment. The ability to survive shocks and protect personnel and equipment has the highest priority. To achieve adequate protection related to vibration and shocks, it is important to have good understanding of shock and vibration mechanics and to have knowledge of the impact of shock and vibration on actual equipment. To reduce the devastating effects of shock and vibrations, suitable dampers are used.

The focus of the current work, is devoted to shock-response, including a theoretical study of the effects of the most common models for shock and vibration dampers. The damping quality of four common rubber damper models is studied.

Here, linear dampers are mostly considered, but in the real world, the assumption of small amplitudes are not always valid. Therefore a section is devoted to the effect of nonlinear stiffness. This effect occurs when a damper is compressed to its limit. This leads to extreme accelerations implying a very high destruction potential.

The report is finalized with a study of the Frahm damper, also called the *tuned mass damper* and its effect in a parallel shock damping system.

Sammendrag

Mekaniske vibrasjoner og sjokk kan være ødeleggende for militært utstyr. Derfor er demping av vibrasjoner og sjokk av stor relevans for militære systemer. Vibrasjoner kan forårsake materialtretthet. Vibrasjoner kan også generere lyd som i sin tur kan avsløre tilstedeværelsen av skip eller kjøretøy. Akustisk "stealth" er en særdeles viktig egenskap for undervannsbåter.

Sjokk fra våpen kan ødelegge militært utstyr. Overlevelsesevnen for sjokk for personell og utstyr har høyeste prioritet. For å oppnå adekvat beskyttelse relatert til vibrasjoner og sjokk er det viktig å ha kunnskap om sjokk og vibrasjonsmekanikk, og effekten av sjokk og vibrasjoner på aktuelt utstyr. For å redusere virkningen av sjokk og vibrasjoner, benyttes tilpassede dempere.

Denne studien omfatter en teoretisk studie av effekten av de mest vanlige sjokk- og vibrasjonsdempere. Demperekvaliteten for fire vanlige gummimodeller blir studert.

Studiet omfatter hovedsakelig lineære modeller, men i den virkelige verden er ikke amplituder alltid små og antagelsen om linæritet bryter da sammen. Derfor er et avsnitt i rapporten viet effekten av ikkelineær stivhet. Denne effekten opptrer når en demper presses til grensen. Dette fører til ekstreme akselerasjoner og et høyt skadepotensial.

Arbeidet avsluttes med et studie av Frahm-demperen som også kalles *the tuned mass damper* og dennes effekt. Her diskuteres denne demperen satt inn i et parallelt sjokkdempingsystem.

Contents

Summary	3
Sammendrag	4
1 Introduction	7
1.1 Presentation of damper models	8
1.2 Example: Differences in action of parallel and serial dampers	9
2 Damper models	11
2.1 The parallel damper model	12
2.2 The serial damper model	12
2.3 The combined damper model	14
2.4 The standard damper model	14
2.5 Harmonically excited support systems, phase relations	16
3 The double half-sine shock	17
3.1 Shock excitation: Double half-sine support motion, examples	17
4 Effects of the four damper models on SRS	19
4.1 Equations for calculation of SRS, parallel model	19
4.2 Equations for calculation of SRS, serial model	20
4.3 Equations for calculations of SRS, combined model	21
4.4 Equations for calculations of SRS, standard model	21
4.5 Results, comparison of the models, varying dissipation.	26
4.6 Results, soft dampers $Q=5$, comparison with stiffer dampers.	29
4.7 Results, comparison of the models with $Q = 5$ and selected values of α, β .	30
5 Nonlinear dampers	31
5.1 Harmonic excitation, nonlinear stiffness	31
5.2 Double half-sine excitation, nonlinear stiffness	33
5.3 Double half-sine excitation, nonlinear stiffness and SRS	33
6 The Frahm damper and its effect on SRS	39
7 Conclusion	42
Appendix	
A Matlab form of the damper equations	43
A.1 Parallel damper model	43
A.2 Serial damper model	43
A.3 Combined damper model	44

A.4	Standard damper model	44
B	Equations for SRS of dampers on matlab form	46
B.1	SRS model for parallel damper	46
B.2	SRS model for serial damper	46
B.3	SRS model for the combined damper	47
B.4	SRS model for the standard damper	47
B.5	Matlab implementation, Frahm damper	48
C	Matlab code for calculating SRS for the parallel damper, example parallel damper	49
	References	53

1 Introduction

After being inspired at meetings at NDMA Naval Systems Division (FMA-markap), and being introduced to the needs in the project P6346, a study of shock response was initiated at FFI. Results of a preliminary study was summarized in [1]. As the collaboration with FMA-markap was strengthened, a need to study a potential degradation of rubber dampers came up among other topics. The study presented in this report was initiated as a result of that need.

The initial goal was to come up with a test-plan for rubber-dampers, but that required better understanding of rubber-dampers in general. A theoretical work on the effect of the most common rubber-damper models on *shock response spectra* (SRS) was then started. As far as the author is aware, such a study has not been previously undertaken or documented in the open literature.

Models of four different dampers, *parallel*, *serial*, *combined* and *standard* were constructed with a support motion system representing the shock, see figure (2.1) in section (2). These models consist of sets of ordinary differential equations, solved numerically. In most cases, the model equations are linear, but an interesting and relevant case including nonlinear stiffness (shocks involve large amplitudes) is treated in section (5).

The damper models studied here, involve multi-parameter problems with combinations in stiffnesses and damping far beyond the scope and limitations of this work. Only the most obvious parameter settings and combinations are covered. Mostly, the combination where the stiffness $k_1 = k_2 = k$ is treated, see comparison in section (4.5), but a case where $k_1 \neq k_2$ is also treated, see section (4.7). The conclusion is that for $k_{\text{parallel}} = k_1 = k_2$, the *combined* and *standard* damper models perform close to the *parallel* damper model, while the *serial* damper model performs better in the sense that the accelerations become smaller. But, this implies need for larger retarding space which may be a drawback. The *serial* damper is unable to handle static forces which makes it less useful. It is possible to tune $k_1 \neq k_2$ for better damping, as shown in section(4.7).

The nonlinear damper model treated in section (5) include the effect of nonlinear stiffness. Nonlinearity in dissipation as occurring for example in van der Pol's equation $\ddot{x} + c(1 - x^2)\dot{x} + x = 0$ is appealing to mathematicians but not studied here. Interesting but not relevant here, nonlinear dissipation can lead to chaotic solutions. For van der Pol's equation, chaotic solutions and limit cycles see [6].

The effect of nonlinearity in stiffness is striking. The purpose of this model is to demonstrate what is going on when a damper is brought into or close to its extreme compression. An increase in stiffness with compression, in particular a strong increase at extreme compression, is applied for example in shock absorbers in vehicles. The strong increase in mechanical stiffness is a necessity for reducing the damage when large amplitude oscillations or shocks occur. On the other hand, the strong response in acceleration particularly at high frequencies also has a damaging potential. The effect of increased stiffness with compression has a dramatic impact to the SRS as is demonstrated in section (5). During the process of designing a shock damping system, it is of the greatest importance that the dampers are designed in such a way that they will never reach a level of compression beyond their capability.

The goal here is to investigate theoretically the quality of dampers through simulated SRS. Single component dampers are mostly treated, but better damping can potentially be achieved by a combination of dampers. The work presented here is accomplished by a study of the *Frahm damper* or *tuned mass damper* which consists of an additional mass absorbing energy, see [3] or the discussion in [5]. (As far as the author is aware, the effect of the tuned mass damper on shocks with the resulting SRS has not been published anywhere else.) The Frahm damper has successfully been applied to many vibration problems including stabilizing the Taipei 101 building, see [7]. It is a passive simple damper which has been applied to systems driven by harmonic forces. Here the shocks studied consist of a double half-sine pulse which is not harmonic. It is not obvious how the Frahm damper works on shocks. This study shows that the Frahm damper may reduce the accelerations in the SRS by a factor of two, see section (6), depending on how it is tuned.

1.1 Presentation of damper models

Dampers are used to isolate and reduce vibrations and shocks for example in vehicles or machine mountings. Tuned mass dampers are used to damp oscillations in bridges and sky scrapers. An remarkable and exotic example of its use, is Taipei 101, a 501 m high sky scraper built in Taipei in the hostile environment of Taiwan which is exposed to both earthquakes and typhoons. This mass damper consists of big dash pots for heat dissipation and a 726 tons spherical pendulum having 0.24% of the total building mass. Due to this damper, Taipei 101 still exists after 18 years of typhoons and earth-quakes. For details see [7]. The number of applications are enormous. Dampers are extensively used in military equipment.

Example of dampers are:

- Wire dampers
- Rubber dampers
- Rubber dampers with internal springs
- Hydraulic dampers
- Tuned dampers

The aforementioned dampers are mostly passive and here only passive dampers are considered, but just to mention it, adaptive/active damper systems exist where feedback loops are used to control vibration. Such dampers are even used in luxury cars. An introduction of vibration dampers and active control is given in [4].

Theory of and characterization of rubber and rubber dampers are described in [2]. A variety of rubber dampers are manufactured by Paulstra-industry, see [9]. In their product catalog, the dampers are characterized by natural frequencies, radial and axial, and by amplification factor at resonance (which is the same as the quality factor Q). For rubber-dampers, typically $Q = 5$.

There are several damper models covering vibration and shock dampering. In this report, four linear visco-elastic damper models are considered: The *parallel*, which in the literature is called the Voigt damper, the *serial* also called Maxwell damper and the dampers here called the *combined* and the *standard* damper. The models treated in this report are presented in table (1.1) and in detail in figure (2.1), consist of combinations of dashpots and springs. To gain insight into how these dampers work, simulations or analytic solutions can help.


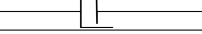
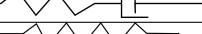
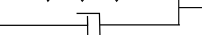
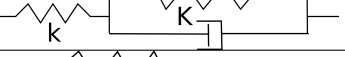

Rubber model	Geometry	Governing equation
Hooke		$m\ddot{x} + kx = 0$
Newton		$m\ddot{x} + c\dot{x} = 0$
Maxwell (serial)		$m\ddot{x} + m(k/c)\dot{x} + kx = 0$
Voigt (parallel)		$m\ddot{x} + c\dot{x} + kx = 0$
Standard linear		$m\ddot{x}_1 + (m(k + K)/c)\dot{x}_1 + kx_1 + (Kk/c)x_1 = 0$
Combined linear		$m\ddot{x}_1 + (mk/c)\dot{x}_1 + (K + k)x_1 + (Kk/c)x_1 = 0$

Table 1.1 Most common damper models

Support excitation through the *double half-sine* pulse is applied throughout this report. This pulse-form is mostly applied in naval applications. SRS are calculated for the four models treated here. In addition, SRS are calculated for the nonlinear model and the Frahm damper model.

It is expected that the damper models behave differently also when they consist of the same material. The damping behavior depends on the construction of the damper. As an example, the damping strength vary proportional to the material damping for a parallel damper, while it varies inversely with the same parameter for the serial damper. The serial damper seems very efficient but it has no “restoring force”. As a consequence it is of limited use since it can not handle static loads and does not have the ability to regain its initial state after impact. It could be used to damp horizontal shocks and vibrations when static load is not an issue and there are other measures to bring the system back to initial state. The other dampers handle static loads.

When it comes to characterization of dampers, quantities like stiffness k , mass (or equivalent mass) m , damping parameters c or ζ with quality factor $Q = 1/2\zeta$, are basic parameters that define the behavior of the damper. These quantities should be derivable for real systems from measurements for example in shakers, shock machines or from stress-strain test machines. Such tests will be considered in a later report.

1.2 Example: Differences in action of parallel and serial dampers

Consider a serial and a parallel damper with the same mass m , damping c and stiffness k , see figure 2.1. Both dampers are excited by an external force. In this case in form of a rectangular pulse. Results are shown in figure (1.1). The governing equations are

$$m\ddot{x} + c\dot{x} + kx = F(t), \quad (1.1)$$

$$m\ddot{x} + (mk/c)\dot{x} + kx = F(t). \quad (1.2)$$

These equations have the same form, but there is a radical difference which implies huge impact on the solutions. Notice that the damping in (1.1) is c , while the damping in (1.2) is mk/c . In figure (1.1) the solutions for the same c , m and k are shown. The solutions are radically different. The *parallel* system shows a gradually decreasing oscillatory behavior while the *serial* system is critically damped.

The governing equations with solutions will be discussed in detail in section (2). Equations (1.1) and (1.2) can be written in a more convenient form

$$\ddot{x} + 2\zeta\omega_n\dot{x} + \omega_n^2x = f(t), \quad \text{parallel} \quad (1.3)$$

$$\ddot{x} + 2\eta\omega_n\dot{x} + \omega_n^2x = f(t), \quad \text{serial} \quad (1.4)$$

where the damping parameters ζ and η are introduced, where $2\zeta\omega_n = c/m$ and $2\eta\omega_n = k/c$. Here, ζ is proportional to c , while η is inversely proportional to c . Particular solutions of equations (1.3) and (1.4) are of the form

$$x = e^{-\zeta\omega_n t} e^{i\omega_n \sqrt{1-\zeta^2} t} \quad (1.5)$$

$$x = e^{-\eta\omega_n t} e^{i\omega_n \sqrt{1-\eta^2} t} \quad (1.6)$$

Consider dampers made of the same material (same c, m and k). Low quality factor Q means high damping. Consider the parallel and serial systems with same c , then $2\zeta\omega_n = c/m$, $2\eta\omega_n = k/c$, $\Rightarrow 2\eta \cdot 2\zeta = 1$. Now $Q_p = 1/(2\zeta)$, $Q_s = 1/(2\eta) \Rightarrow Q_p = 1/Q_s$. Clearly Q_s and Q_p are inversely proportional. The two systems damping is different. The only exception is $Q = 1$.

On the other hand let the two systems have the same damping and natural frequency. Then $2\zeta\omega_n = 2\eta\omega_n \Rightarrow c_p c_s = km = c_c^2/4$, where c_c is the critical damping parameter. Then they have in general different damping parameters. The only case of equality is when $c_p = c_s = c_c/2$.

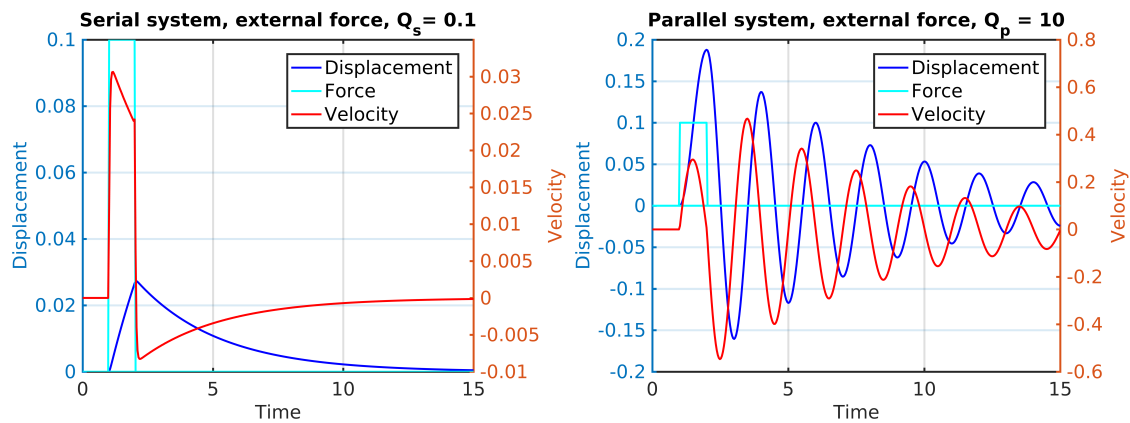


Figure 1.1 Oscillations excited by a rectangular pulse. Left figure, serial configuration. Right figure, parallel configuration. Both with same material damping parameter c , mass m and stiffness k .

2 Damper models

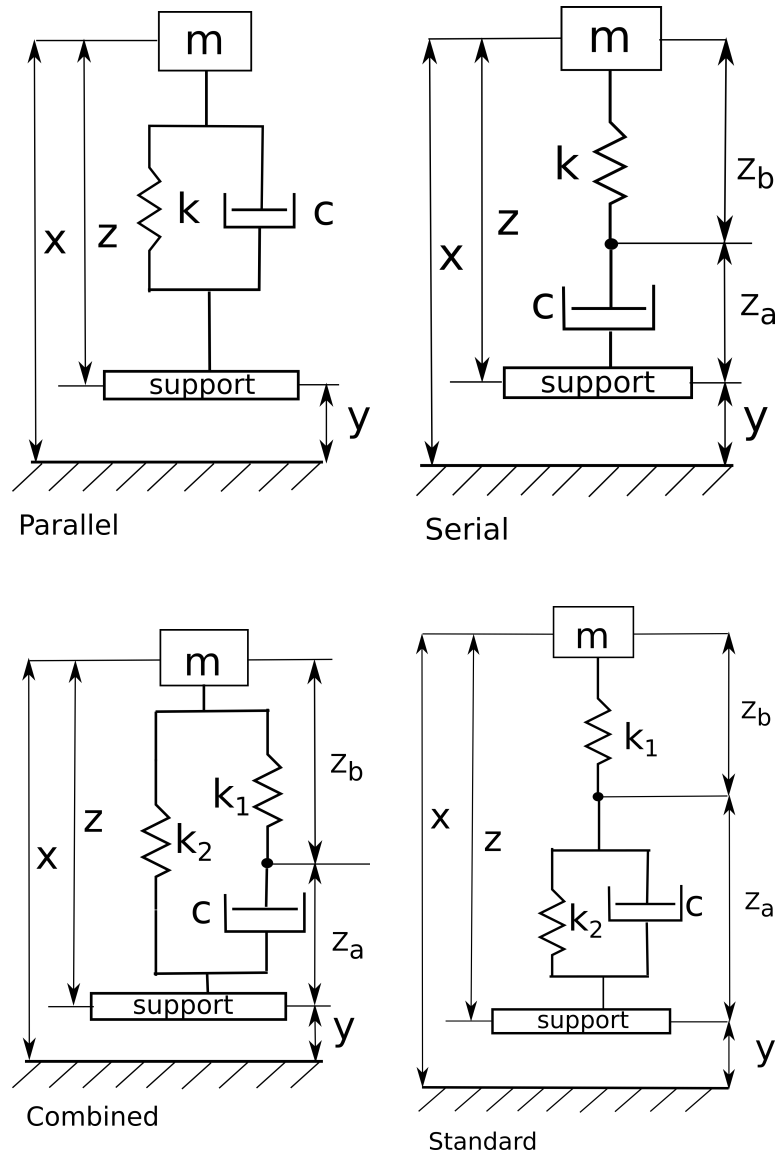


Figure 2.1 Simple damper models

The theory of rubber is treated among others in [2], but how rubber dampers handle shocks is not treated there. The shock models handled here are based on systems of support motion expressed y , \dot{y} and \ddot{y} . Some examples consisting of harmonic support motion, but most effort is devoted to the double half-sine shock which is defined according to the expressions (3.1), (3.2) and (3.3) in section (3). The motivation is naval shocks.

2.1 The parallel damper model

Consider the parallel damper model shown in figure (2.1) upper left. It consists of a spring and dashpot set up in parallel, following [8], using $x = y + z$, the sum of forces acting on the mass m are given by the linear equation

$$m\ddot{x} = -c\dot{z} - kz \Rightarrow \ddot{z} + (c/m)\dot{z} + (k/m)z = -\ddot{y}, \quad (2.1)$$

where m is mass, c is the damping coefficient and k is the stiffness of the spring. Introducing $2\zeta\omega_n = k/c$ and $\omega_n^2 = k/m$ gives

$$\ddot{z} + 2\zeta\omega_n\dot{z} + \omega_n^2z = -\ddot{y}, \quad (2.2)$$

where ω_n is the natural frequency and ζ is the dimensionless damping, $\zeta = c/\sqrt{mk} = c/c_c$. If $\zeta \geq 1$, the oscillations are critically damped. ζ also affects the frequency of the oscillator which is $\omega = \omega_n\sqrt{1 - \zeta^2}$.

To get a better feel for the consequences of support motion excitation, harmonic excitation is treated first. Let $y = \sin \omega t$, $\dot{y} = \omega \cos \omega t$, $\ddot{y} = -\omega^2 \sin \omega t$. In the numerical examples, $t \geq 0$. To well pose the problem, initial conditions are needed.

At $t = 0$, assume $x(0) = 0$, $\dot{x}(0) = 0$. Since $x = y + z$, $z(0) = 0$ and using $\dot{x} = \dot{y} + \dot{z}$, it follows that $\dot{z}(0) = -\omega$. The acceleration is

$$\ddot{x} = -2\zeta\omega_n\dot{z} - \omega_n^2z$$

implying $\ddot{x}(0) = 2\zeta\omega\omega_n$.

Results of harmonic excitation for both parallel and serial systems are shown in figure (2.2). For matlab implementation see (A.1).

2.2 The serial damper model

The sum of forces acting on m , see figure (2.1) upper right, are $m\ddot{x} = -kz_b = -c\dot{z}_a$, with $z = z_a + z_b$, $x = z_a + z_b + y$. Using $m\ddot{x} = -kz_b$ yields

$$m(\ddot{z}_a + \ddot{z}_b + \ddot{y}) = -kz_b, \quad \Rightarrow \quad \ddot{z}_b + (k/c)\dot{z}_b + (k/m)z_b = -\ddot{y}.$$

Notice the term k/c which imply the counter intuitive result that low viscosity leads to high damping. The reason for this is as follows. The force on m is directed through the dashpot as $m\ddot{x} = -c\dot{z}_a$, the same force is directed through the spring $-kz_b$. For low viscosity, \dot{z}_a is big and the ‘‘compressibility’’ of the dashpot becomes big, reducing acceleration and implying high damping. The damping parameter for the serial system is denoted η . ($2\eta\omega_n = k/c$, for the parallel system ζ given by $2\zeta\omega_n = c/m$). The derivations above lead to the following equation

$$\ddot{z}_b + 2\eta\omega_n^2\dot{z}_b + \omega_n^2z_b = -\ddot{y}. \quad (2.3)$$

On the other hand, using $m\ddot{x} = -c\dot{z}_a$, yields

$$\ddot{z}_a + 2\eta\omega_n\dot{z}_a + \omega_n^2z_a = -2\eta\omega_n\dot{y}. \quad (2.4)$$

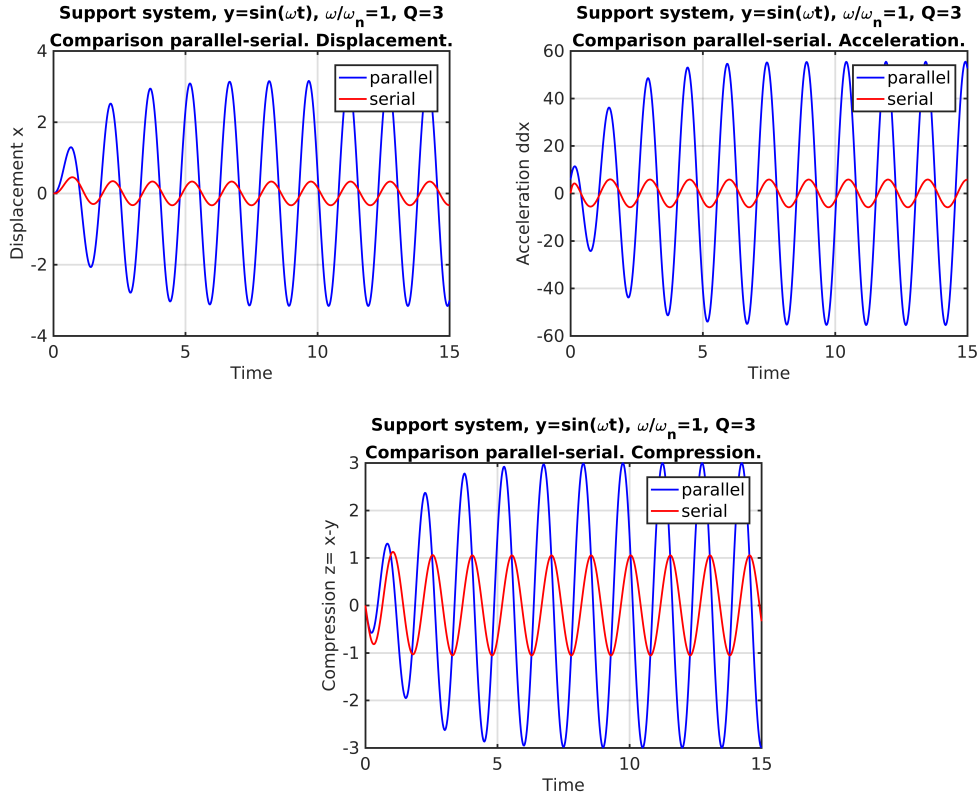


Figure 2.2 Comparison parallel and serial harmonic support motion.

Adding equations (2.3) and (2.4) gives

$$\ddot{z} + 2\eta\omega_n\dot{z} + \omega_n^2z = -(\ddot{y} + 2\eta\omega_n\dot{y}), \quad (2.5)$$

which alternatively can be written

$$\ddot{z} + (k/c)\dot{z} + (k/m)z = -(\ddot{y} + (k/c)\dot{y}), \quad (2.6)$$

Compare the parallel and the serial system i.e. equations (2.2) and (2.5). The viscosity appears differently in the two systems. The force term due to the motion of the support, contains for the serial system $2\eta\omega_n\dot{y}$ in addition to \ddot{y} . Its contribution is inversely proportional to c . This makes a difference. Small $c \Rightarrow \eta$ large. It is evident from equation (2.5) that $\dot{z} \approx -\dot{y}$. As the viscosity is small, the motion of m : $\dot{x} = \dot{y} + \dot{z}$, is small. Nearly all energy is absorbed in the dashpot.

Initial conditions, serial damper with harmonic excitation:

As for the parallel system but in addition assuming $z_a = z_b = x = 0$ at $t = 0$. Assuming also $\dot{x} = 0$, $\dot{x} = \dot{y} + \dot{z} \Rightarrow \dot{z} = -\dot{y}$. Since $z_a = z_b = 0$, and $c\dot{z}_a = k\dot{z}_b \Rightarrow \dot{z}_a = 0$, then $\dot{z}_b = -\dot{y} = -\omega$ at $t = 0$.

The acceleration for the serial system is:

$$\ddot{x} = -2\eta\omega_n\dot{x} - \omega_n^2z = -\omega_n^2z_b, \quad \Rightarrow \quad \ddot{x}(0) = 0, \quad (2.7)$$

which differs from the parallel system.

Examples of systems excited by harmonic support motion are shown in figures (2.2), (2.3) and (2.4). For matlab implementation see (A.2)

2.3 The combined damper model

The combined damper model is depicted in figure (2.1), lower left. The sum of forces acting on m is

$$m\ddot{x} = -k_2z - k_1z_b = -k_2z - c\dot{z}_a,$$

$x = y + z_a + z_b$, and $c\dot{z}_a = k_1z_b$. Substitution gives

$$\ddot{z}_b + (k_1/c)\dot{z}_b + (k_1/m + k_2/m)z_b = -(k_2/m)z_a - \ddot{y}_b$$

which gives the system

$$\dot{z}_a = 2\eta\omega_1z_b, \quad (2.8)$$

$$\ddot{z}_b + 2\eta\omega_1\dot{z}_b + (\omega_1^2 + \omega_2^2)z_b = -\ddot{y} - \omega_2^2z_a, \quad (2.9)$$

where the angular frequencies and damping parameter η are given as

$$\omega_1^2 = k_1/m, \quad \omega_2^2 = k_2/m, \quad 2\eta\omega_1 = k_1/c.$$

Examples of harmonic excitation of the combined model is shown in figures (2.3), (2.4).

Combined model, initial conditions, harmonic excitation:

At $t = 0$, $x(0) = 0 \Rightarrow z(0) = 0$ and assuming $z_b(0) = 0 \Rightarrow z_a(0) = 0$, $\dot{z}_a(0) = 0$. Finally $\dot{x}(0) = 0 \Rightarrow \dot{z}_b(0) + \dot{y}(0) = 0 \Rightarrow \dot{z}_b(0) = -\dot{y}$.

The initial acceleration is $\ddot{x}(0) = -(\omega_1^2 + \omega_2^2)z_b(0) - \omega_2^2z_a(0) = 0$.

The governing equations for the combined model can be written as follows:

$$\dot{z}_a = 2\eta\omega_1z_b,$$

$$\dot{z}_b = \xi,$$

$$\dot{\xi} = -2\eta\omega_1\xi - (\omega_1^2 + \omega_2^2)z_b - \omega_2^2z_a - \ddot{y}.$$

For matlab implementation, see section (A.3).

2.4 The standard damper model

The standard damper model is shown in the lower right panel in figure (2.1). The sum of forces acting on m is:

$$m\ddot{x} = -k_1z_b = -(k_2z_a + c\dot{z}_a) \Rightarrow$$

$$\dot{z}_a = (k_1/c)z_b - (k_2/c)z_a, \quad (2.10)$$

$$\ddot{z}_b + (k_1/c)\dot{z}_b + (k_1/m - k_1k_2/c^2)z_b = -(k_2/c)^2z_a - \ddot{y}, \quad (2.11)$$

where $2\eta_1\omega_1 = k_1/c$, $2\eta_2\omega_2 = k_2/c$, $\omega_1^2 = k_1/m$, $\omega_2^2 = k_2/m \Rightarrow \eta_2 = (\omega_2/\omega_1)\eta_1 \Rightarrow$.

$$\dot{z}_a = 2\eta_1\omega_1(z_b - (\omega_2/\omega_1)^2 z_a), \quad (2.12)$$

$$\ddot{z}_b + 2\eta_1\omega_1\dot{z}_b + \omega_1^2(1 - (2\eta_1\omega_2/\omega_1)^2)z_b = -\ddot{y} - \omega_2^2(2\eta_1\omega_2/\omega_1)^2 z_a. \quad (2.13)$$

Standard damper, harmonic forcing:

Assuming initial conditions $x = 0$, $\dot{x} = 0$, $y = 0$, $\dot{y} = \omega$, $z_a = z_b = 0$, since $c\dot{z}_a = k_1z_b - k_2z_a$, $\dot{z}_a = 0$, $\dot{z}_b = -\omega$.

Diagnostics:

$$\begin{aligned} x &= z_a + z_b + y, \\ \dot{x} &= 2\eta_1\omega_1(z_b - (\omega_2/\omega_1)^2 z_a) + \dot{z}_b + \dot{y}, \\ \ddot{x} &= -\omega_1^2 z_b. \end{aligned}$$

The matlab form of equations for the standard model can be found in (A.4)

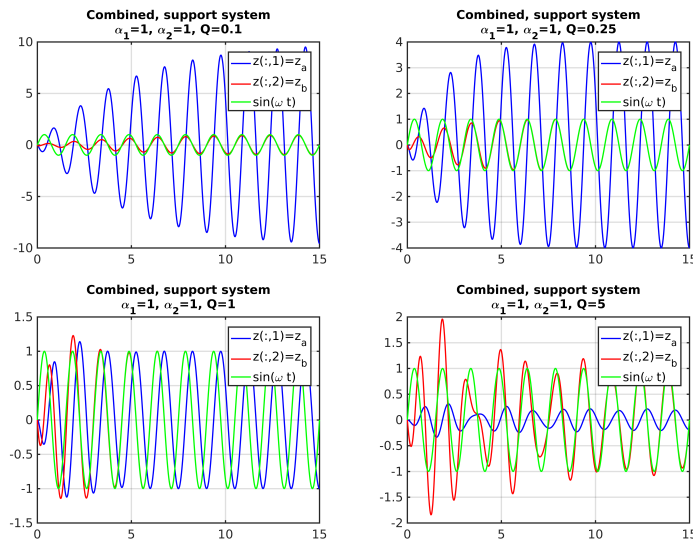


Figure 2.3 Results of harmonic excitation of support system for combined damper and for various Q .

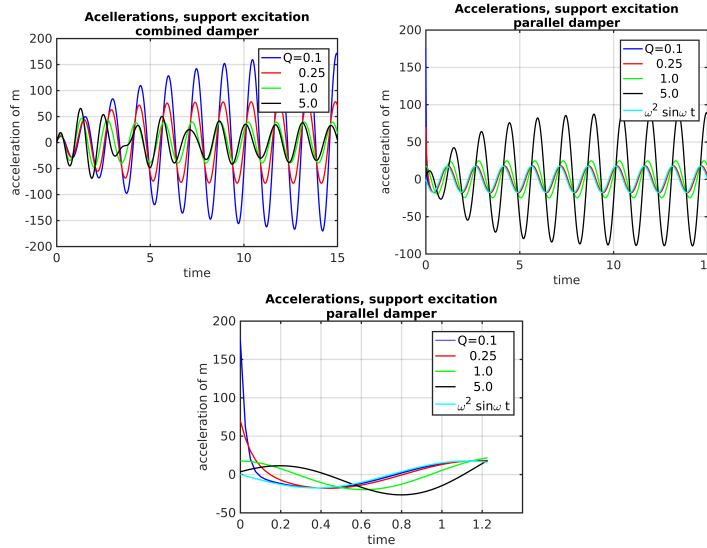


Figure 2.4 Acceleration of mass caused by harmonic excitation of support system. Combined damper, parallel damper, various Q .

2.5 Harmonically excited support systems, phase relations

Let $y = y_0 \sin \omega t$, and the response be $z = z_0 \sin(\omega t - \phi)$. For the parallel system, substitution into equation (2.2) gives for the phase

$$\tan \phi = \frac{2\zeta(\omega/\omega_n)}{1 - (\omega/\omega_n)^2},$$

For the serial system, substitution into equation (2.5) gives

$$\tan \phi = \frac{2\eta(\omega_n/\omega)}{1 - (\omega/\omega_n)^2 - (2\eta)^2}.$$

Notice the inverse ω_n/ω in the last expression. At resonance, for the parallel system $\phi = \pi/2$, while for the serial system the phase angle depends on the damping, $\tan \phi = -1/(2\eta) = -Q$. A very simple and interesting result! Since $2\eta\omega_n = k/c$, $Q = \omega_n(c/k)$. For small c , $\tan \phi \rightarrow -0, \Rightarrow \phi \rightarrow \pi$. In this case, there is no transfer of force between the support and mass. The support moves as y and $y = -z$, confirming that $\phi \rightarrow \pi$.

3 The double half-sine shock

The initial conditions for the shock are $x(0) = 0, \dot{x}(0) = 0$. The initial state for the support is $y(0) = 0, \dot{y} = 0$, so since $x = y + z, z(0) = 0, \dot{z}(0) = 0$. The shock is designed such that the support velocity after the shock is zero ($\int_0^{t_2} \ddot{y} dt = \int_0^{t_1} \ddot{y} dt + \int_{t_1}^{t_2} \ddot{y} dt = 0$). Let A be the amplitude of the first part of the pulse. The shock used in this report has form as a double half-sine function in acceleration given as

$$\ddot{y}(t) = A \begin{cases} \sin \frac{\pi}{t_1} t, & 0 \leq t \leq t_1, \\ -\frac{t_1}{t_2-t_1} \sin \frac{\pi(t-t_1)}{t_2-t_1}, & t_1 < t \leq t_2, \\ 0, & t_2 < t. \end{cases} \quad (3.1)$$

$$\dot{y}(t) = A \frac{t_1}{\pi} \begin{cases} 1 - \cos \frac{\pi}{t_1} t, & 0 \leq t \leq t_1, \\ 1 + \cos \frac{\pi(t-t_1)}{t_2-t_1}, & t_1 < t \leq t_2. \\ 0, & t_2 < t, \end{cases} \quad (3.2)$$

$$y(t) = A \frac{t_1}{\pi} \begin{cases} t - \frac{t_1}{\pi} \sin \frac{\pi}{t_1} t, & 0 \leq t \leq t_1, \\ t + \frac{t_2-t_1}{\pi} \sin \frac{\pi(t-t_1)}{t_2-t_1}, & t_1 < t \leq t_2, \\ t_2, & t_2 < t. \end{cases} \quad (3.3)$$

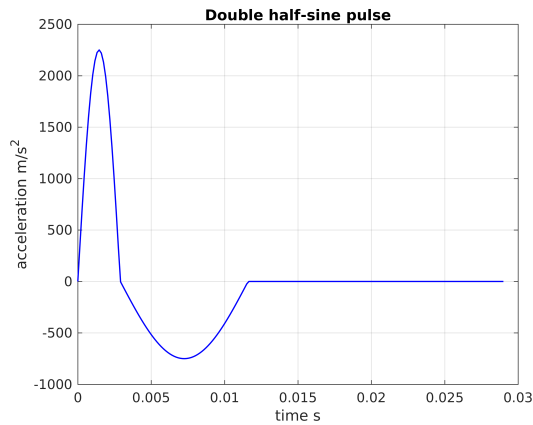


Figure 3.1 The figure shows a double half-sine pulse defined by $A = 2250\text{m/s}^2, t_1 = 0.0029\text{s}, t_2 = 0.0116\text{s}$

3.1 Shock excitation: Double half-sine support motion, examples

To get some feel of the four damper models response of the double half-sine excitation, solutions are plotted for the case $Q = 5$. In figure (3.2), acceleration, velocity, displacement of mass and distance between support and mass are shown as function of time. The plots are for the same ω and damping c . Evidently the models respond differently and the SRS can be expected to be different for the various models as shown later in this report. Notice that the acceleration of mass is smaller for the *serial* damper as the change in distance between support and mass become more larger. More space is needed to avoid collision between mass and support compared with the other

dampers. The *standard* damper also acts different compared with the parallel and combined dampers. Its dissipation is less than the others.

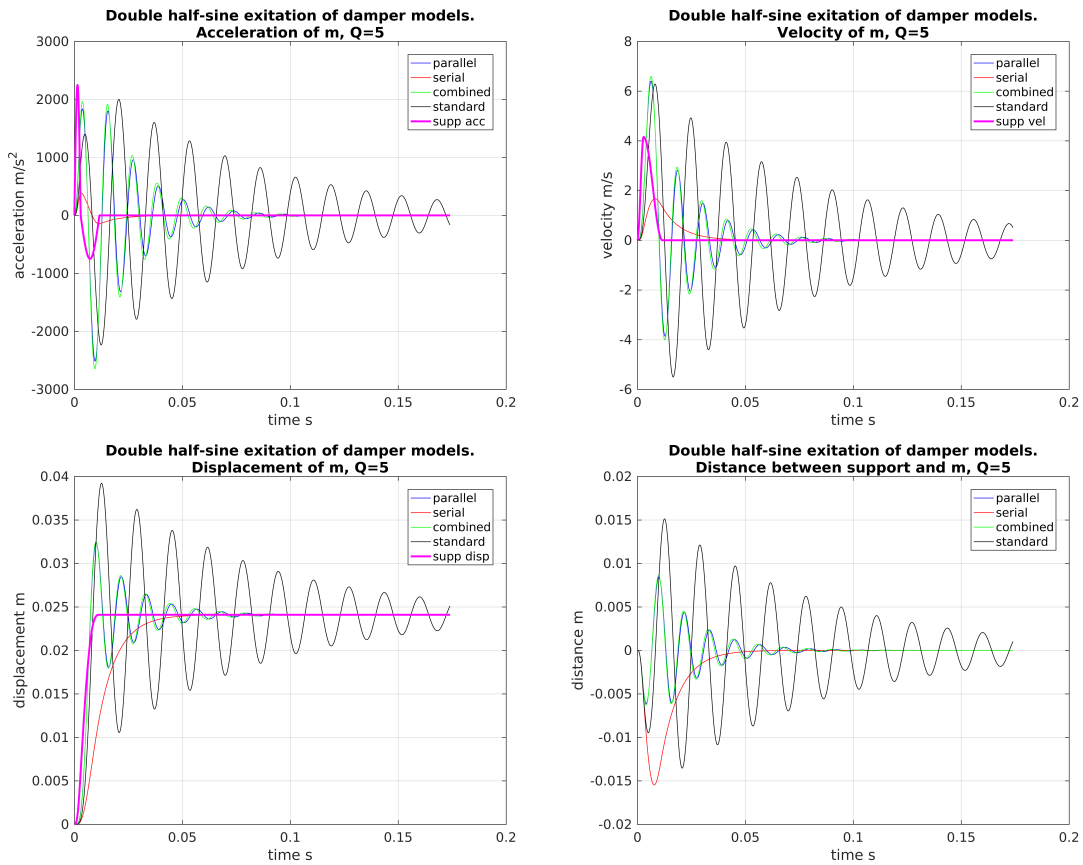


Figure 3.2 The four models excited by a double half-sine shock. For $Q = 5$, same ω and c , acceleration, velocity, displacement and distance between support and mass are shown as function of time.

4 Effects of the four damper models on SRS

SRS is calculated by adding a SRS-probe to the system. This is shown in figure (4.1). When calculating the SRS, it is assumed that the mass of the probe is much smaller than that of the system to be analyzed, $\mu = m_p/m \ll 1$ and the probes have no influence on the motion of the system to be analyzed. In this section the equations for arbitrary μ is developed, but when running the simulations, $\mu \ll 1$. Matlab forms of the equations are summarized in appendix (A).

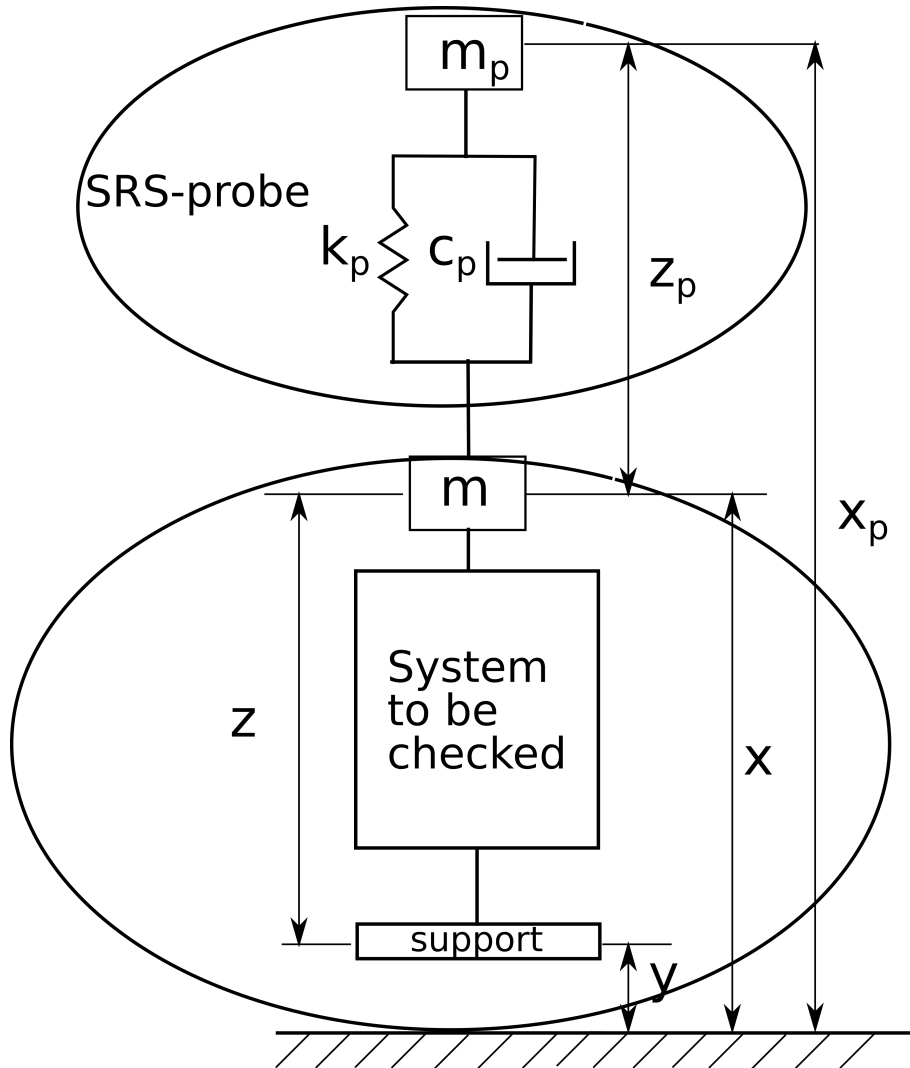


Figure 4.1 The figure shows a system with the SRS-probe attached

4.1 Equations for calculation of SRS, parallel model

Consider the forces working on mass m_p and m for the parallel system as shown in figures (4.1) and (2.1). Now $x = z + y$, $x_p = x + z_p = z + z_p + y$. Also $\mu = m_p/m$, $\omega^2 = k/m$, $\omega_p^2 = k_p/m_p$, and

$2\zeta\omega = c/m$, $2\zeta_p\omega_p = c_p/m_p$. The sum of forces on m_p and m are

$$m_p\ddot{x}_p = -k_p z_p - c_p \dot{z}_p, \quad (4.1)$$

$$m\ddot{x} = -kz - c\dot{z} + k_p z_p + c_p \dot{z}_p. \quad (4.2)$$

Equation 4.1 implies

$$\ddot{z}_p + 2\zeta_p\omega_p\dot{z}_p + \omega_p^2 z_p = -\ddot{x},$$

which is the equation of a damped oscillator with support motion expressed by \ddot{x} . To close the problem, the interaction between m and m_p is taken into consideration which gives the following equations

$$\ddot{z} + 2\zeta\omega\dot{z} + \omega^2 z - 2\zeta_p\omega_p\mu\dot{z}_p - \omega_p^2\mu z_p = -\ddot{y}. \quad (4.3)$$

$$\ddot{z}_p + 2\zeta_p\omega_p(1 + \mu)\dot{z}_p + \omega_p^2(1 + \mu)z_p - 2\zeta\omega\dot{z} - \omega^2 z = 0, \quad (4.4)$$

The accelerations become

$$\ddot{x}_p = -2\zeta_p\omega_p\dot{z}_p - \omega_p^2 z_p, \quad (4.5)$$

$$\ddot{x} = -2\zeta\omega\dot{z} - \omega^2 z + 2\zeta_p\omega_p\mu\dot{z}_p + \omega_p^2\mu z_p, \quad (4.6)$$

4.2 Equations for calculation of SRS, serial model

Consider the serial model with the forces acting on m_p and m , see figures 4.1 and 2.1. The sum of forces at the SRS-probe m_p is caused by the spring k_p and the dashpot c_p . The forces acting on mass m are from m_p through the spring k_p and dashpot c_p , and from the spring k which equals the force from the dashpot c , so $c\dot{z}_a = kz_b$. This implies

$$m\ddot{x} = -kz_b + c_p\dot{z}_p + k_p z_p, \quad (4.7)$$

$$m_p\ddot{x}_p = -c_p\dot{z}_p - k_p z_p. \quad (4.8)$$

With $x_p = x + z_p$, equation (4.8) implies

$$\ddot{z}_p + 2\zeta_p\omega_p\dot{z}_p + \omega_p^2 z_p = -\ddot{x},$$

which shows that m_p acts as an SRS probe for the support motion \ddot{x} of m .

Now $x = z_a + z_b + y \Rightarrow \ddot{x} = \ddot{z}_a + \ddot{z}_b + \ddot{y}$, and $\ddot{z}_a = (k/c)\dot{z}_b$, substitution in equations (4.7) and (4.8) gives

$$\ddot{z}_b + \frac{k}{c}\dot{z}_b + \frac{k}{m}z_b = -\ddot{y} + \frac{c_p}{m}\dot{z}_p + \frac{k_p}{m}z_p, \quad (4.9)$$

$$\ddot{z}_p + \frac{c_p}{m_p}\dot{z}_p + \frac{k_p}{m_p}z_p = -\ddot{x} = -\left(-\frac{k}{m}z_b + \frac{c_p}{m}\dot{z}_p + \frac{k_p}{m}z_p\right). \quad (4.10)$$

The accelerations can be written

$$\ddot{x} = -\omega^2 z_b + 2\zeta_p\omega_p\mu\dot{z}_p + \omega_p^2\mu z_p,$$

$$\ddot{x}_p = -2\zeta_p\omega_p\dot{z}_p - \omega_p^2 z_p.$$

The governing equations become

$$\dot{z}_a = 2\eta\omega z_b, \quad (4.11)$$

$$\ddot{z}_b + 2\eta\omega\dot{z}_b + \omega^2 z_b - 2\zeta_p\omega_p\mu\dot{z}_p - \omega_p^2\mu z_p = -\ddot{y}, \quad (4.12)$$

$$\ddot{z}_p + 2\zeta_p\omega_p(1 + \mu)\dot{z}_p + \omega_p^2(1 + \mu)z_p = \omega^2 z_b, \quad (4.13)$$

where $\mu = m_p/m$, $\omega = \sqrt{k/m}$, $\omega_p = \sqrt{k_p/m_p}$, $2\eta\omega = k/c$, $2\zeta_p\omega_p = c_p/m_p$.

4.3 Equations for calculations of SRS, combined model

The combined model with SRS probe is obtained by replacing the box in figure 4.1 with the lower left panel of figure 2.1. Force balance implies

$$\begin{aligned} m_p\ddot{x}_p &= -c_p\dot{z}_p - k_p z_p, \\ m\ddot{x} &= -k_2 z - k_1 z_b + c_p\dot{z}_p + k_p z_p = -k_2 z - c\dot{z}_a + c_p\dot{z}_p + k_p z_p. \end{aligned}$$

$x = y + z = y + z_a + z_b$, $x_p = x + z_p = y + z + z_p = y + z_a + z_b + z_p$,
 $\mu = m_p/m$, $\omega_1^2 = k_1/m$, $\omega_2^2 = k_2/m$, $\omega_p^2 = k_p/m_p$, $2\zeta_p\omega_p = c_p/m_p$, $2\eta\omega_2 = k_2/c$, implies

$$\ddot{x}_p + 2\zeta_p\omega_p\dot{z}_p + \omega_p^2 z_p = 0, \quad \Rightarrow \quad \ddot{z}_p + 2\zeta_p\omega_p\dot{z}_p + \omega_p^2 z_p = -\ddot{x},$$

showing that m acts as a support system for oscillator m_p .

$$\begin{aligned} m\ddot{x} &= -k_2 z - k_1 z_b + k_p z_p + c_p\dot{z}_p = -k_2 z - c\dot{z}_a + k_p z_p + c_p\dot{z}_p, \\ m_p\ddot{x}_p &= -k_p z_p - c_p\dot{z}_p. \end{aligned}$$

The above equations can be rewritten as

$$\dot{z}_a = 2\eta\omega_1 z_b, \quad (4.14)$$

$$\ddot{z}_b + 2\eta\omega_1\dot{z}_b + (\omega_1^2 + \omega_2^2)z_b - 2\zeta_p\omega_p\mu\dot{z}_p - \omega_p^2\mu z_p = -\ddot{y} - \omega_2^2 z_a, \quad (4.15)$$

$$\ddot{z}_p + 2\zeta_p\omega_p(1 + \mu)\dot{z}_p + \omega_p^2(1 + \mu)z_p = \omega_2^2 z_a + (\omega_1^2 + \omega_2^2)z_b. \quad (4.16)$$

Accelerations

$$\begin{aligned} \ddot{x}_p &= -\omega_p^2 z_p - 2\zeta_p\omega_p\dot{z}_p, \\ \ddot{x} &= -\omega_2^2 z_a - (\omega_1^2 + \omega_2^2)z_b + \omega_p^2\mu z_p + 2\zeta_p\omega_p\mu\dot{z}_p. \end{aligned}$$

4.4 Equations for calculations of SRS, standard model

Consider figures 4.1 and the lower right panel of figure 2.1. The forces acting on m_p and m are

$$\begin{aligned} m_p\ddot{x}_p &= -k_p z_p - c_p\dot{z}_p \quad \Rightarrow \quad m_p\ddot{z}_p + c_p\dot{z}_p + k_p z_p = -m_p\ddot{x}, \\ m\ddot{x} &= -k_1 z_b + c_p\dot{z}_p + k_p z_p = -k_2 z_a - c\dot{z}_a + c_p\dot{z}_p + k_p z_p, \\ k_1 z_b &= k_2 z_a + c\dot{z}_a. \end{aligned}$$

Combining these equations give

$$\dot{z}_a = 2\eta_1\omega_1 \left(z_b - (\omega_2/\omega_1)^2 z_a \right), \quad (4.17)$$

$$\ddot{z}_b + 2\eta_1\omega_1\dot{z}_b + \omega_1^2(1 - (2\eta_1\omega_2/\omega_1)^2)z_b = -\ddot{y} - \omega_2^2(2\eta_1\omega_2/\omega_1)^2 z_a + \omega_p^2\mu z_p + 2\zeta_p\omega_p\mu\dot{z}_p, \quad (4.18)$$

$$\ddot{z}_p + 2\zeta_p\omega_p(1 + \mu)\dot{z}_p + \omega_p^2(1 + \mu)z_p = \omega_1^2 z_b, \quad (4.19)$$

where $\mu = m_p/m$ and

$\omega_1^2 = k_1/m$, $\omega_2^2 = k_2/m$, $\omega_p^2 = k_p/m_p$, $2\zeta_p\omega_p = c_p/m_p$, $2\eta_1\omega_1 = k_1/c$, $2\eta_2\omega_2 = k_2/c$. Define $\alpha = \omega_2/\omega_1 = \sqrt{k_2/k_1}$, then $\eta_2/\eta_1 = \omega_2/\omega_1 = \alpha$.

The accelerations are

$$\begin{aligned} \ddot{x}_p &= -\omega_p^2 z_p - 2\zeta_p\omega_p\dot{z}_p, \\ \ddot{x} &= -\omega_1^2 z_b + \omega_p^2\mu z_p + 2\zeta_p\omega_p\mu\dot{z}_p. \end{aligned}$$

The probe functions for the SRS calculation is shown in figure (4.2) and (4.3). The resulting SRS are shown in figure (4.4).

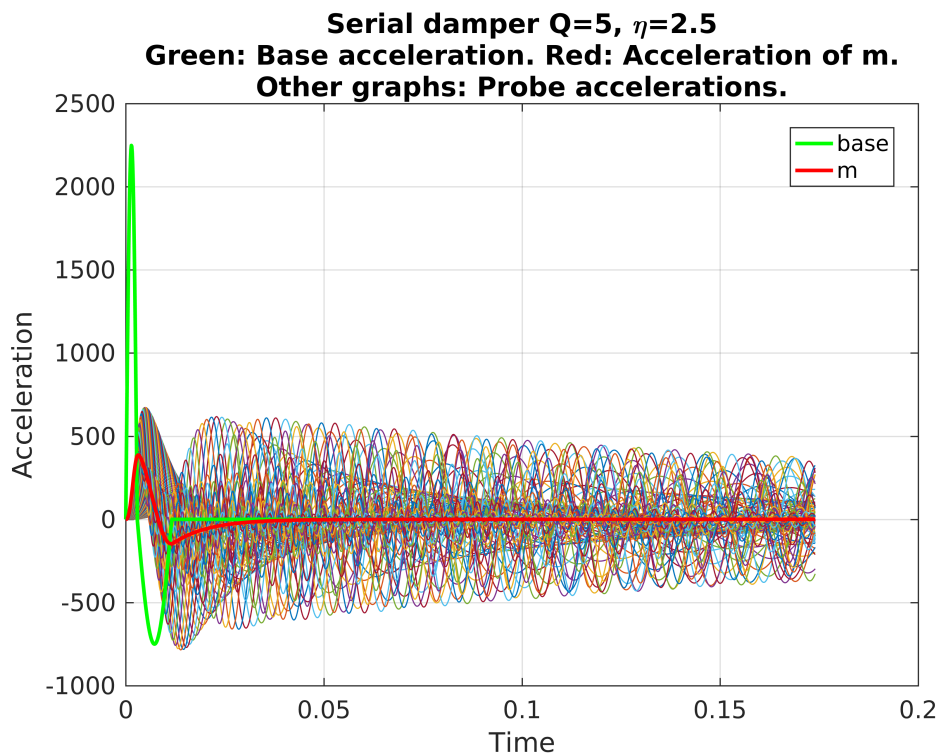
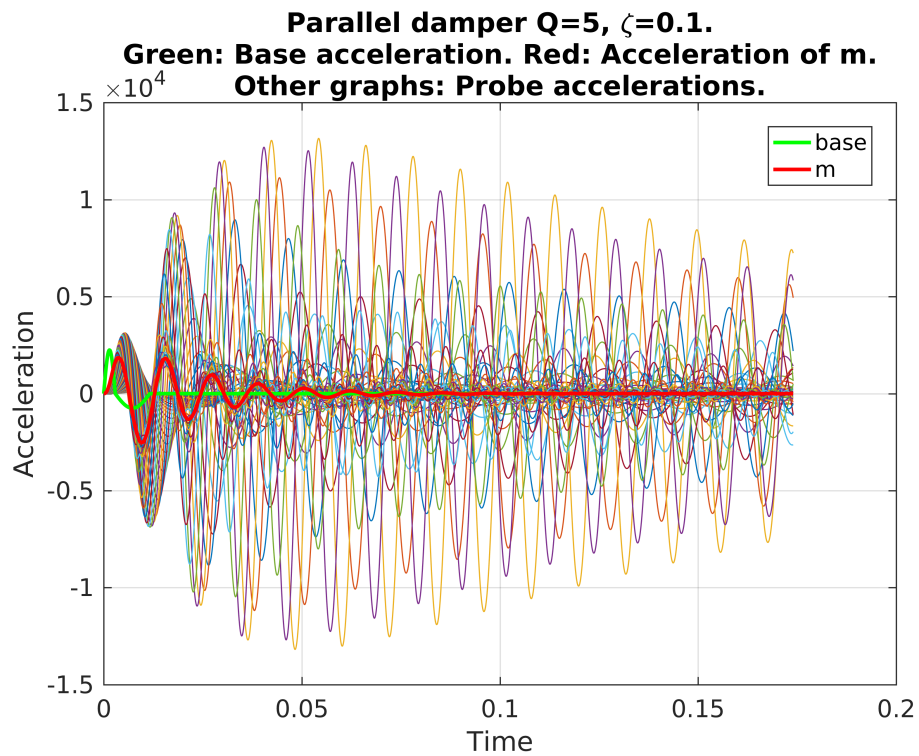


Figure 4.2 Probe functions for the SRS calculations for the parallel and serial models

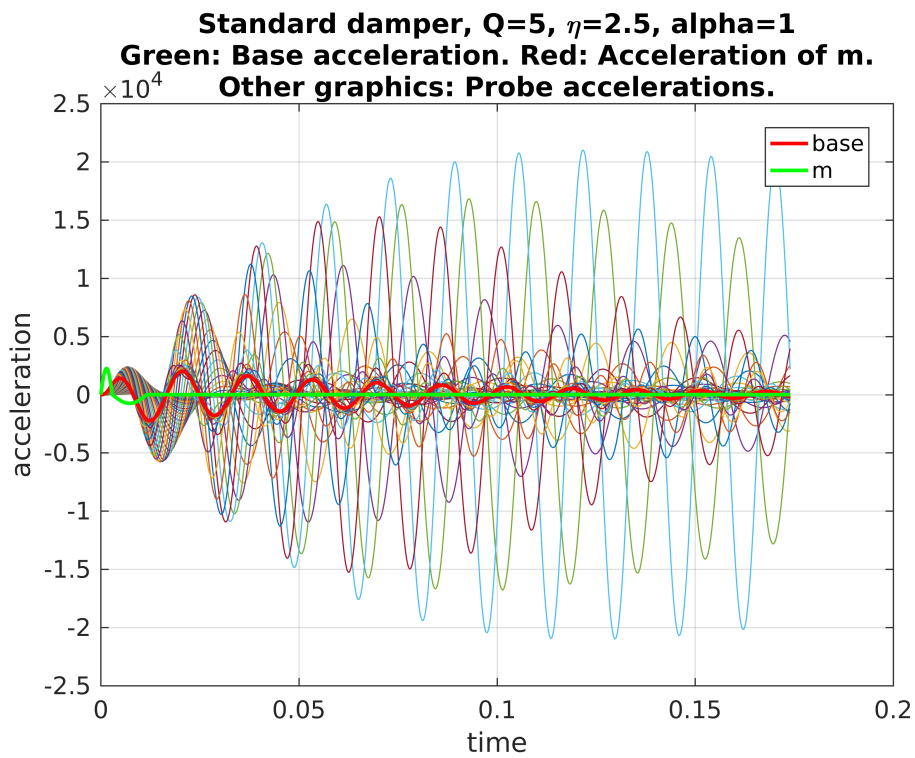
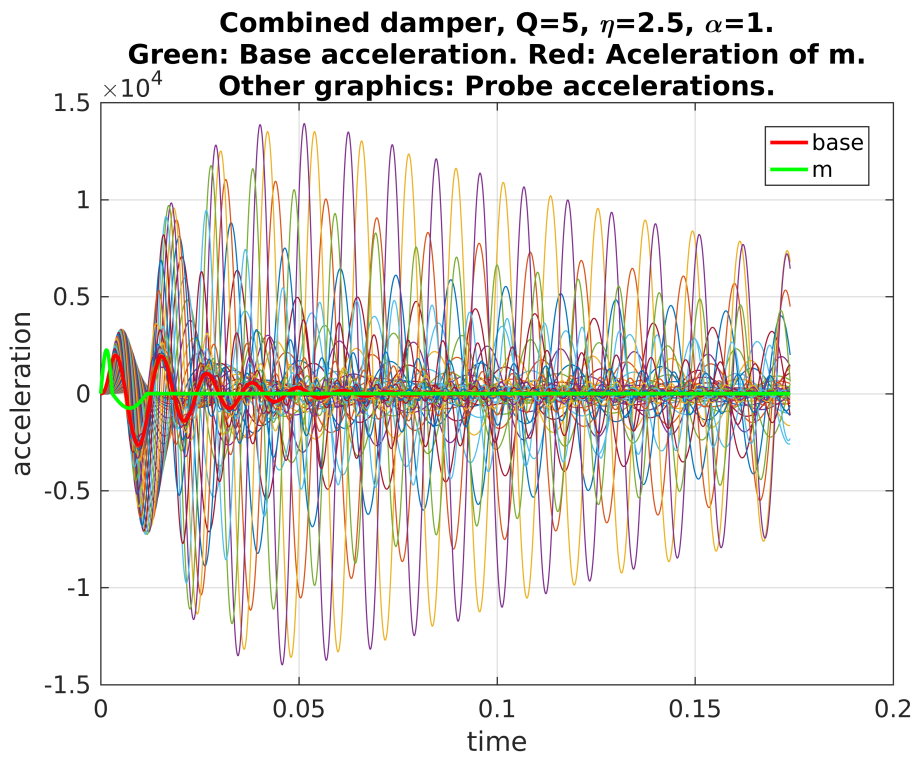


Figure 4.3 Probe functions for the SRS calculations for the combined and standard models

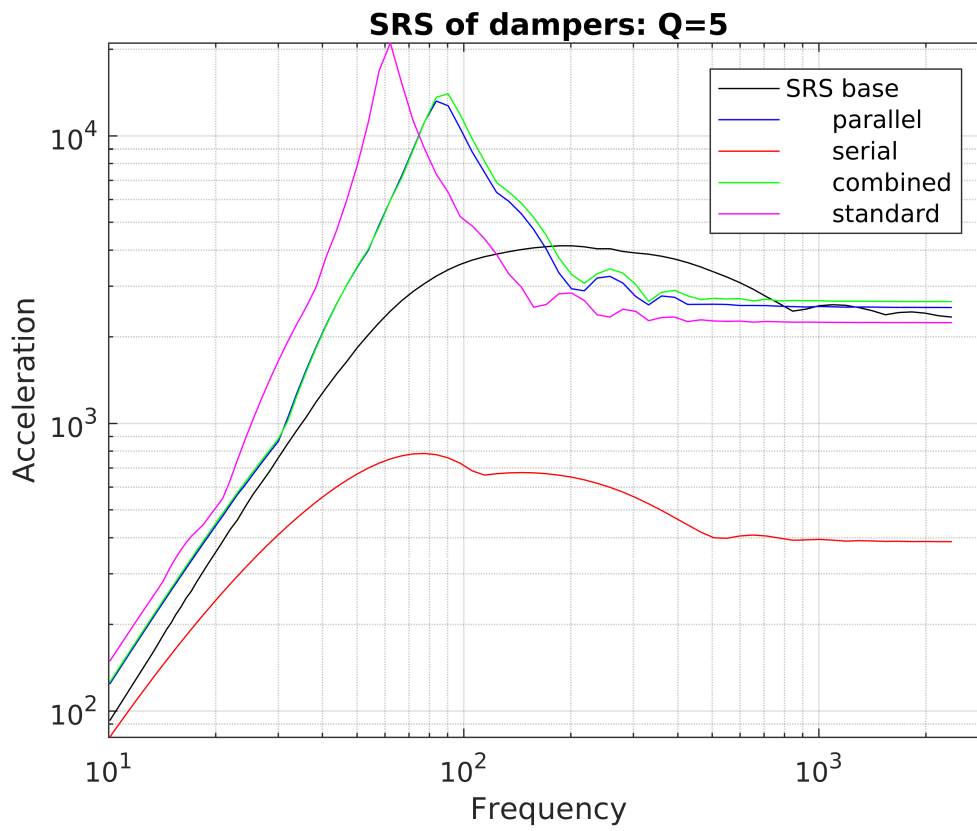


Figure 4.4 SRS for all models $Q=5$.

4.5 Results, comparison of the models, varying dissipation.

To compare the models, the material properties should be the same. The following physical parameters are involved m, k_1, k_2, c . For simplicity let m and c be the same for all models. It could be of interest to investigate the effects of varying k_1 and k_2 , but here the study is limited to the case $k_1 = k_2 = k$. In the parallel model, damping parameter c enters the numerator. In the other models, c enters the denominator (see equations (4.3), (4.4),(4.11),(4.12),(4.17) and (4.18)).

Matlab scripts are developed and applied to the four damper models, see Appendix (A). As an example the matlab code for the parallel case is shown in appendix (C). The simulation results are shown in figures (4.5) through (4.9).

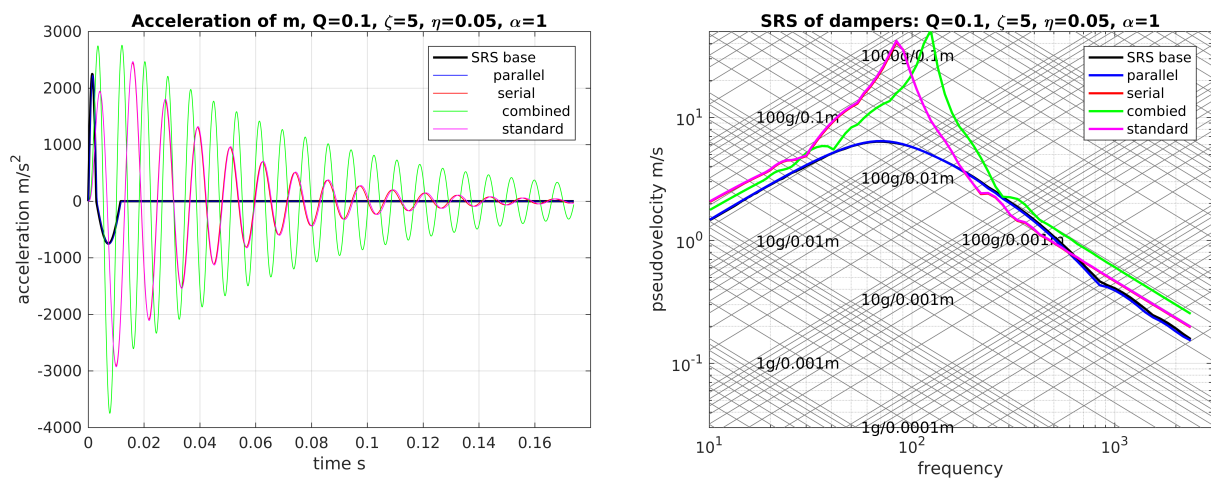


Figure 4.5 SRS for the four damper models, $Q = 0.1$, parallel merges with base, serial merges with standard.

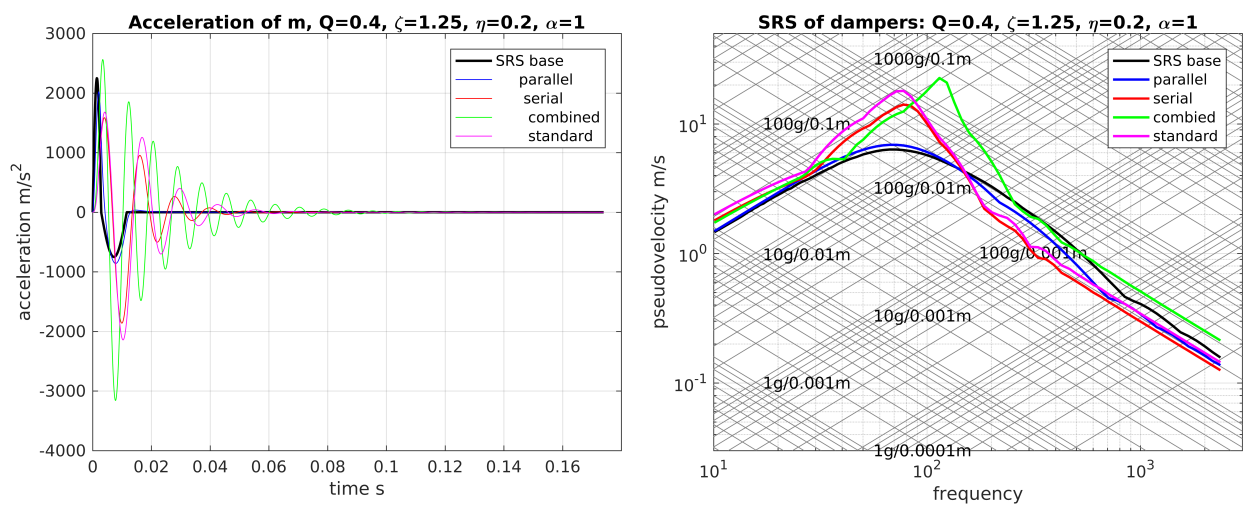


Figure 4.6 SRS for the four damper models, $Q = 0.4$.

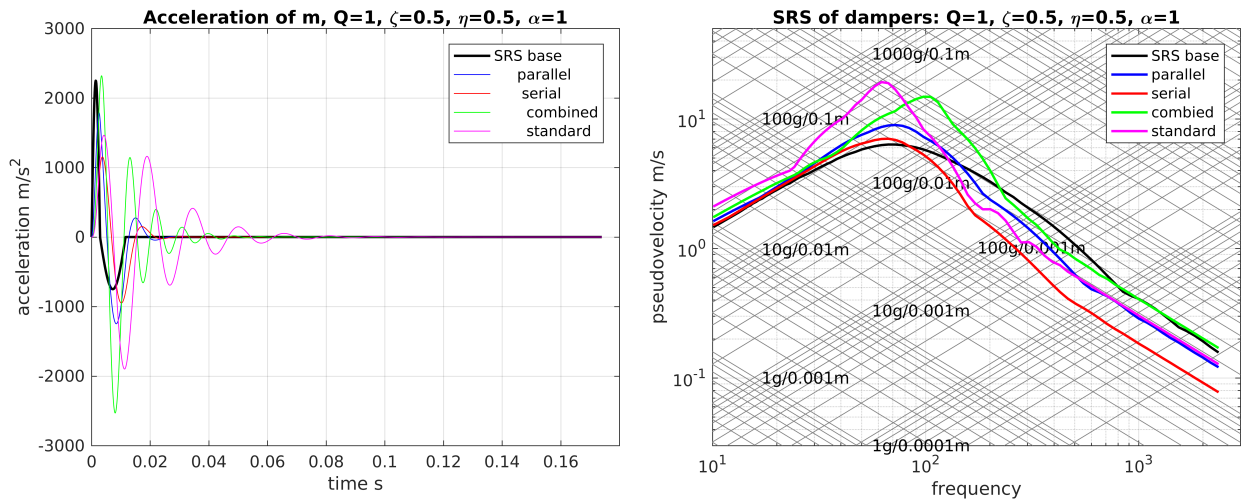


Figure 4.7 SRS for the four damper models, $Q = 1$

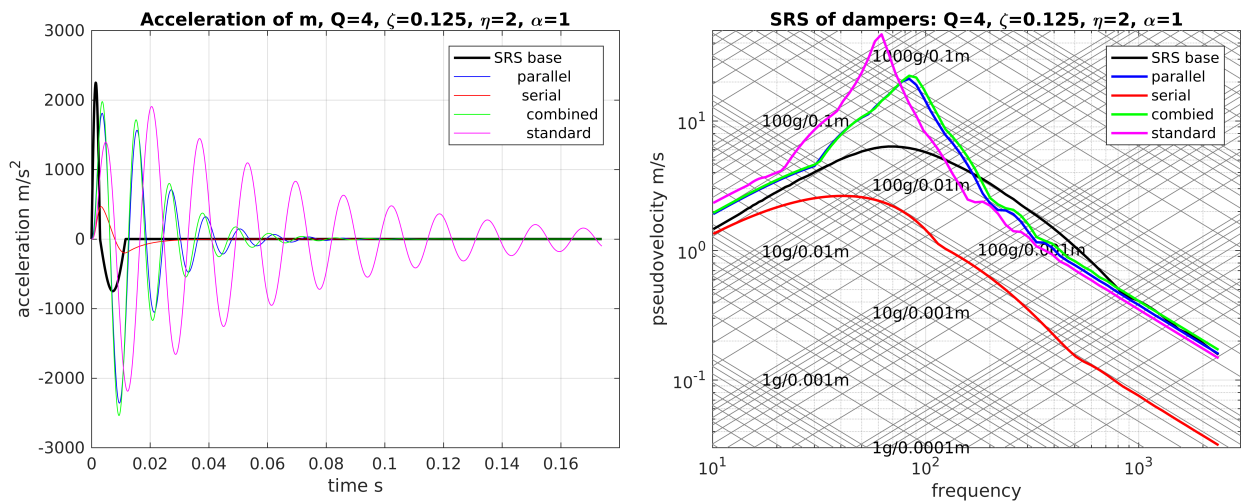


Figure 4.8 SRS for the four damper models, $Q = 4$.

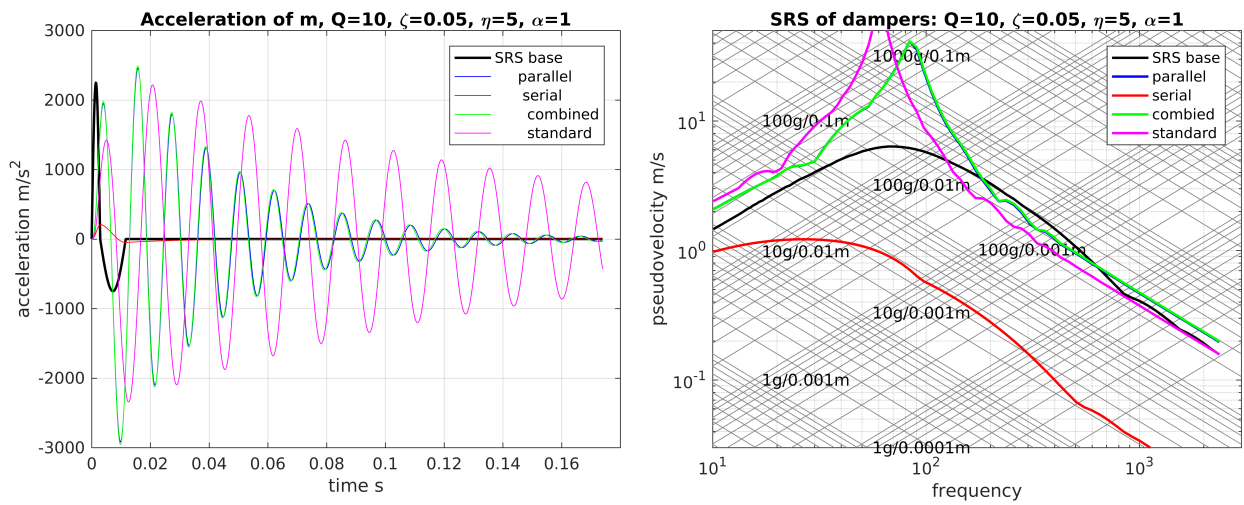


Figure 4.9 SRS for the four damper models, $Q = 10$, parallel merges with combined.

4.6 Results, soft dampers $Q=5$, comparison with stiffer dampers.

Here the stiffness of the dampers are reduced so that the eigen-frequency is reduced from 60 – 80 Hz to 8 – 16 Hz which is a more realistic stiffness for dampers used in real systems. For comparison the results are show in figure (4.10). The softer dampers need room for nearly twice the compression compared with the stiffer ones.

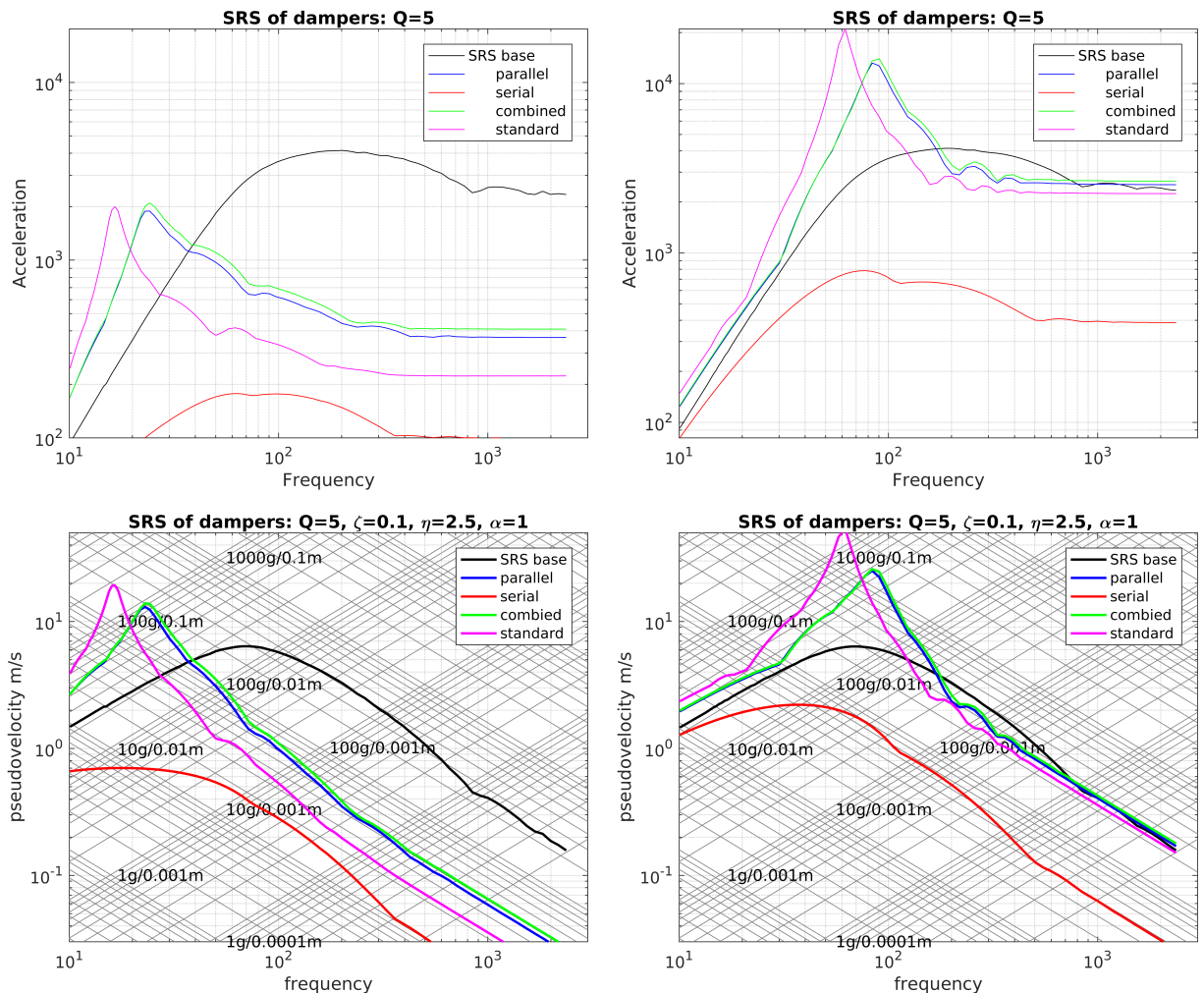


Figure 4.10 SRS for the four damper models, $Q = 5$, for different stiffness. Tripartite plots are shown for comparison. The result of the softer damper systems indicate that the shock is absorbed over nearly twice the compression compared with the stiff system. Room must be reserved for this compression.

4.7 Results, comparison of the models with $Q = 5$ and selected values of α, β .

Dampers should be able to keep static equilibrium. In this section the three dampers *parallel*, *combined* and *standard* are compared. For the parallel and the combined dampers spring k and k_2 support the equilibrium. For the combined damper a parameter $\alpha = \omega_1/\omega_2$ and since k_2 supports equilibrium it is natural to define $\omega_2 = 2\pi \cdot n/T$, defining the natural oscillation of the system. For the standard damper static equilibrium is kept by k , where $1/k = 1/k_1 + 1/k_2$. For this damper let $\Omega = 2\pi \cdot n/T$ defining the natural oscillation of this system. Now introduce β such that the two frequencies $\omega_1 = \beta\Omega$ and $\omega_2 = \beta\Omega/\sqrt{\beta^2 - 1}$, which requires $\beta > 1$. Simulation results with $\alpha = \beta$ are shown in the figures (4.11). It is shown that there are combinations of k_1 and k_2 that give good shock damping.

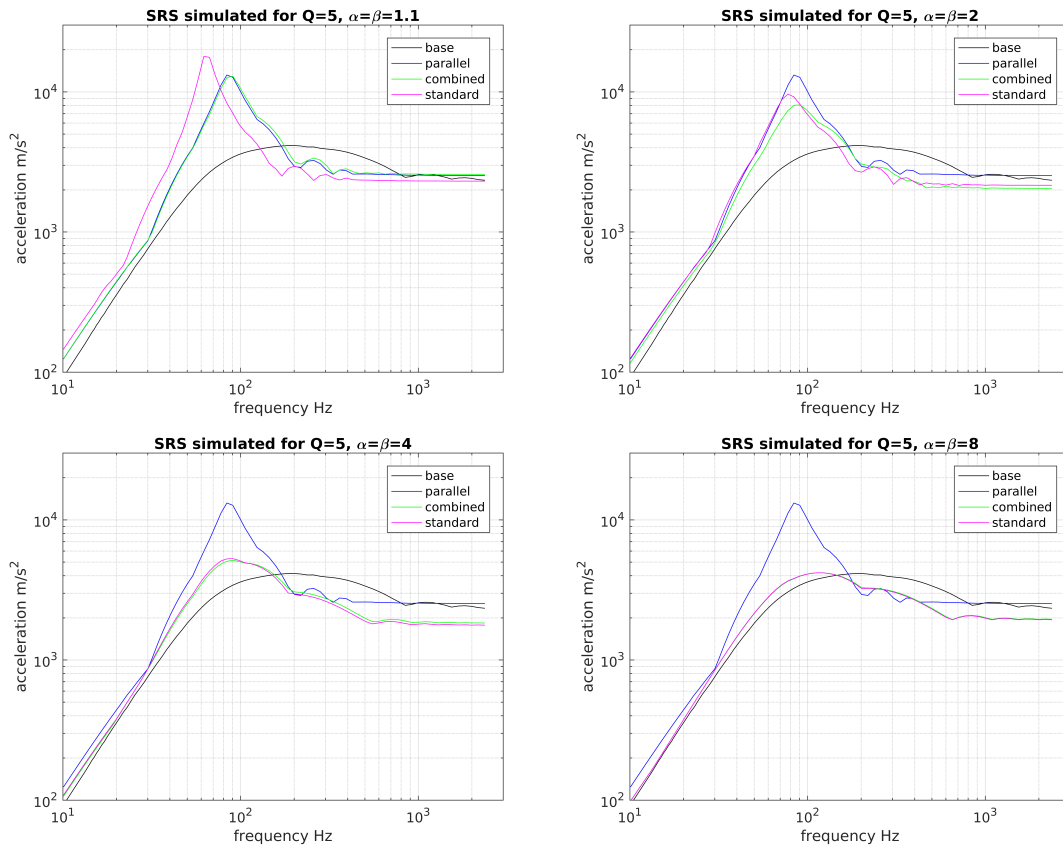


Figure 4.11 SRS for the three damper models, $Q = 5$, for $\alpha = \beta = 1.1, 2.0, 4.0, 8.0$, showing that by letting $k_1 \neq k_2$ it is possible to construct dampers that can handle static equilibrium and as the same time be good shock dampers.

5 Nonlinear dampers

The simplest model of a nonlinear damper has increasing stiffness as a function of contraction/stretching $k = k(\xi)$. In addition it is expected that contraction acts different than stretching. To avoid collision when the spring is nearly maximally compressed, the spring system can be designed such that the stiffness progressively increases with compression. This is seen in some car spring systems where rubber dampers are used to limit the most extreme compression.

Consider a system where the stiffness increases as the damper is compressed while it is constant as it is being stretched. Assume $\alpha > 0$ and n a positive and odd integer. The stiffness can then be written

$$k(\xi) = k_0 o(z) = k_0 \begin{cases} 1, & \text{if } \xi \geq 0, \\ (1 + \alpha(\xi/2\xi_0)^n), & \text{if } \xi < 0. \end{cases} \quad (5.1)$$

The governing equation for the parallel support system is

$$m\ddot{z} + c\dot{z} + k(z)z = -m\ddot{y}. \quad (5.2)$$

Assuming that the damping parameter c is independent of z , this implies

$$\ddot{z} + 2\zeta\omega_0\dot{z} + \omega^2(z)z = -\ddot{y}. \quad (5.3)$$

Here $\omega_0^2 = k_0/m$, $2\zeta\omega_0 = c/m$ and $\omega^2(z) = \omega_0^2 o(z)$. Following the equation for SRS for the parallel oscillator, we obtain for the nonlinear system

$$\ddot{z} + 2\zeta\omega_0\dot{z} + \omega^2(z)z - 2\zeta_p\omega_p\mu\dot{z}_p - \omega_p^2 z_p = -\ddot{y}, \quad (5.4)$$

$$\ddot{z}_p + 2\zeta_p\omega_p(1 + \mu)\dot{z}_p + \omega_p^2(1 + \mu)z_p - 2\zeta\omega_0\dot{z} - \omega^2(z)z = 0. \quad (5.5)$$

5.1 Harmonic excitation, nonlinear stiffness

In all cases below, $Q = 5$.

As an example, consider harmonic forcing with nonlinear response expressed by equation (5.3) with $\ddot{y} = -\omega_0^2 \sin(\omega_0 t)$. The stiffness is given by $k o(z)$, $o(z)$ is shown in figure (5.1), $\omega^2(z) = \omega_0^2 o(z)$. By solving equation (5.3) the acceleration \ddot{x} is accessed and the results are shown in figure (5.1).

The nonlinear stiffness cause distortions in the wave form with sharp peaks in acceleration \ddot{x} . This is caused by increased stiffness as the compression approaches its maximum. This is seen in figure (5.1). As z increases, the wave shape approaches normal (compare with the linear wave shape) until again z goes negative and the same repeats.

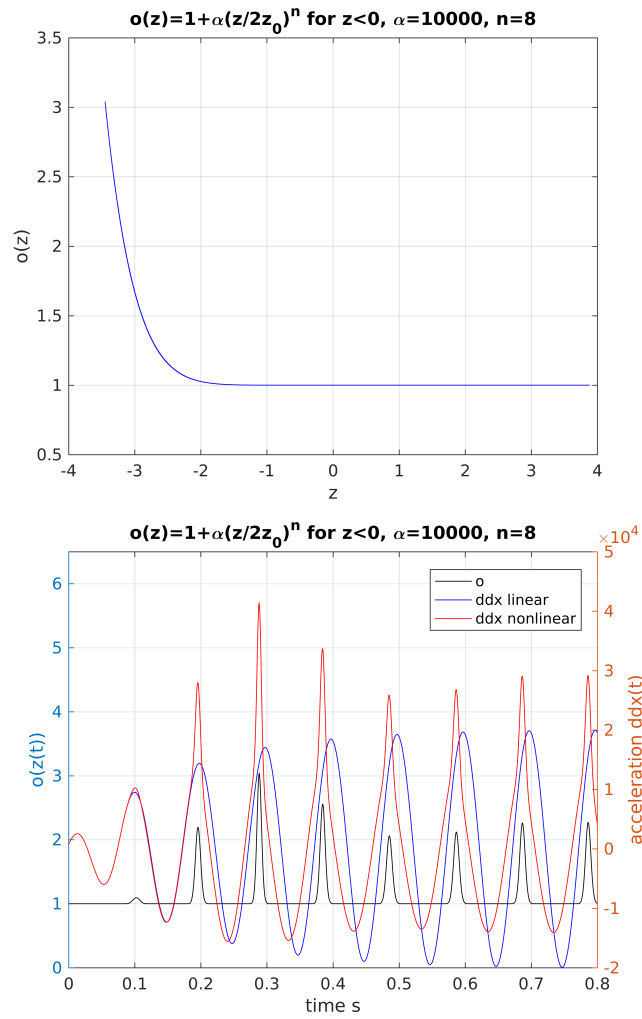


Figure 5.1 Upper panel: The function $o(z) = 1$ for $z \geq 0$ and $o(z) = 1 + \alpha(z/2z_0)^n$ for $z < 0$, compression. The stiffness curve is calculated for harmonic forcing. Lower panel: Nonlinear response to harmonic forcing. The blue curve shows linear response while the red curve shows the nonlinear response. The black curve shows the function: $o(z)$.

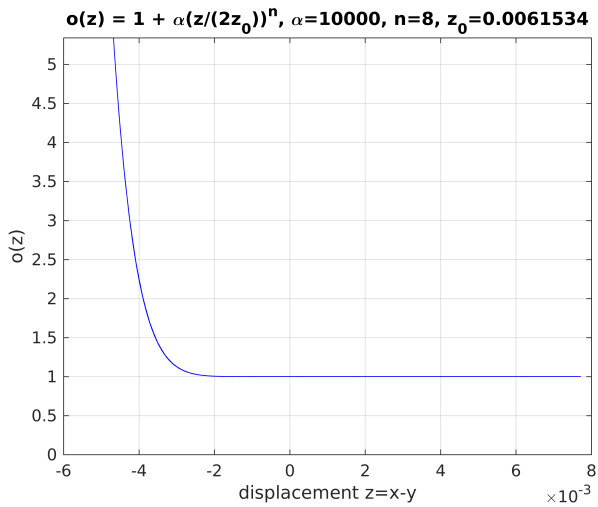


Figure 5.2 The function $o(z) = 1$ for $z \geq 0$ and $o(z) = 1 + \alpha(z/2z_0)^n$ for $z < 0$. The shock profile is a double half-sine

5.2 Double half-sine excitation, nonlinear stiffness

Consider now the double half-sine pulse acting at a support system with a parallel damper. In this case, equation (5.3) is solved with double half-sine excitation as defined previously. The stiffness profile is shown in figure (5.2).

Acceleration $\ddot{x}(t)$ and compression $z(t)$ are shown in figure (5.3).

5.3 Double half-sine excitation, nonlinear stiffness and SRS

Let the support excitation be of the double half-sine form. To calculate the SRS, equations (5.4) and (5.5) are solved. The probe oscillations used to calculate the SRS are shown in figure (5.4)

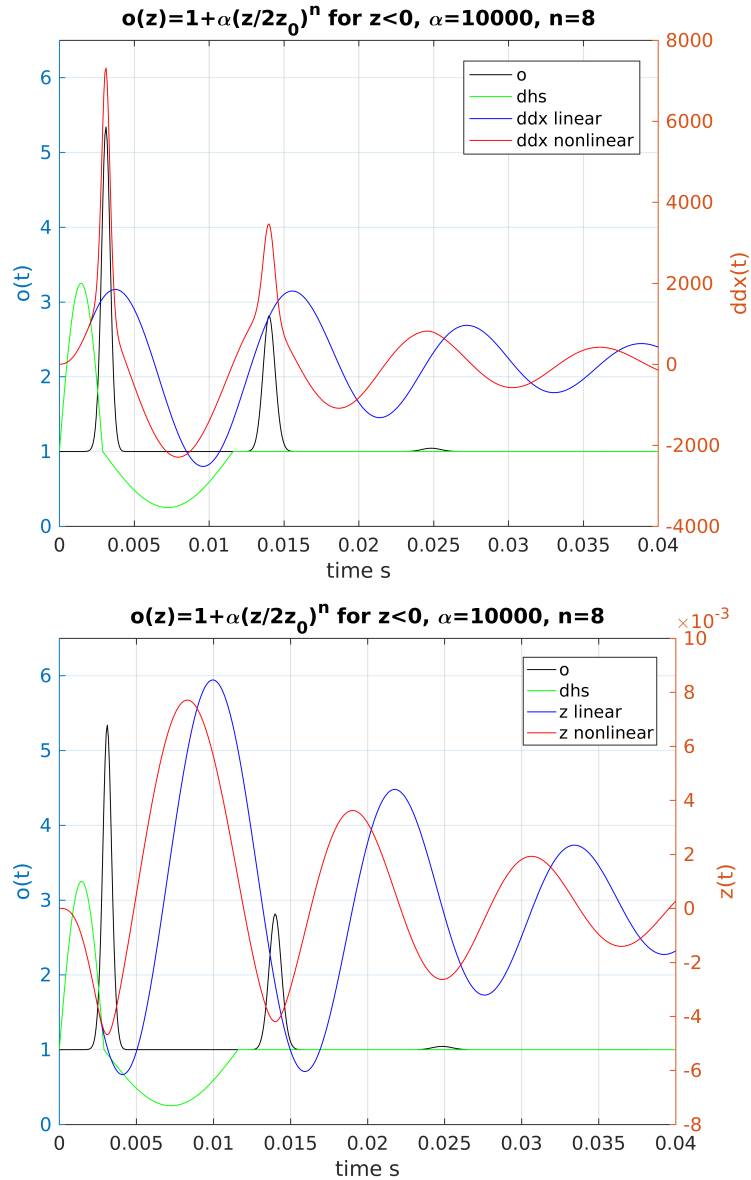


Figure 5.3 Response to a double half-sine pulse showing the difference of linear and nonlinear responses. Accelerations $\ddot{x}(t)$ are shown in the upper plot while compression $z(t)$ are shown in the lower. The blue curves show linear response while the red curves show nonlinear response. Evidently the nonlinear compression is smaller than the linear. The black curves show the nonlinear factor: $o(z)$. The green curves show the double half-sine pulse.

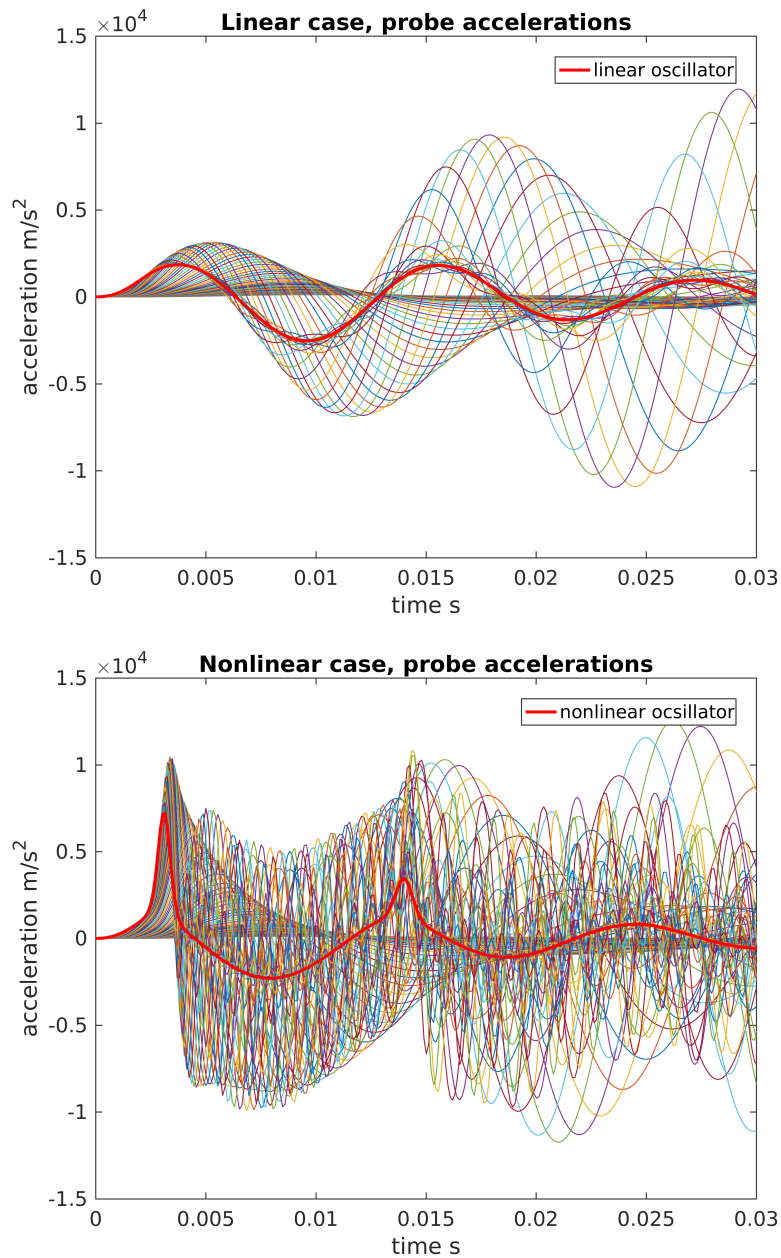


Figure 5.4 These plots show sections of the linear and nonlinear probe functions. Upper plot shows probes for the linear damper model while the lower plot shows the probes for the nonlinear damper model. The linear and nonlinear oscillations are shown by the red curves.

Tripartite plots depend on linearity to be valid. In the nonlinear case, there is not a simple relation between acceleration, pseudo velocity and pseudo displacement and these quantities become meaningless. Spectra of velocity and displacement must be calculated independently as $\max(\text{abs}(\dot{x}))$ and $\max(\text{abs}(x))$. SRS based on acceleration for the current nonlinear damper

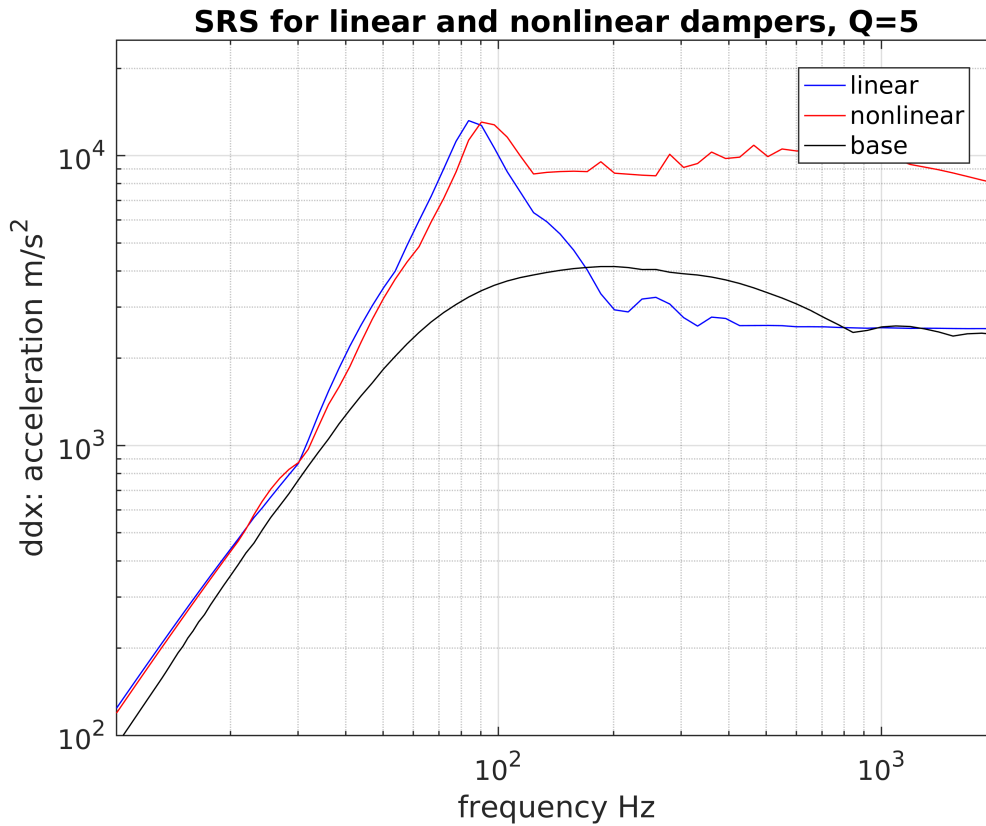


Figure 5.5 Comparison of SRS of a linear and a nonlinear damper. The blue curve shows the SRS for the linear damper while the red curve shows the SRS for the nonlinear damper. The black curve shows the SRS of the double half-sine base motion. These spectra are based on acceleration. Note the high values in the high frequency tail in the spectrum of the nonlinear damper.

described in this section is shown in figure (5.5). A plot of pseudo-velocity $pv(f) = a(f)/(\pi f)$ for the linear and the nonlinear case, shows that the results deviate from the calculated SRS from velocity and displacement-data separate. The deviations are in particular big for the high frequency part of the spectrum, see figure (5.5)

SRS based on velocity \dot{x} and displacement x can be calculated from the algorithms for both the linear and nonlinear dampers. The results are shown in figure (5.6) and (5.7). Since shock criteria for naval applications in many cases are presented as tripartite plots, the comparison with velocity and displacement SRS deserves more attention. This is beyond the scope of this report.

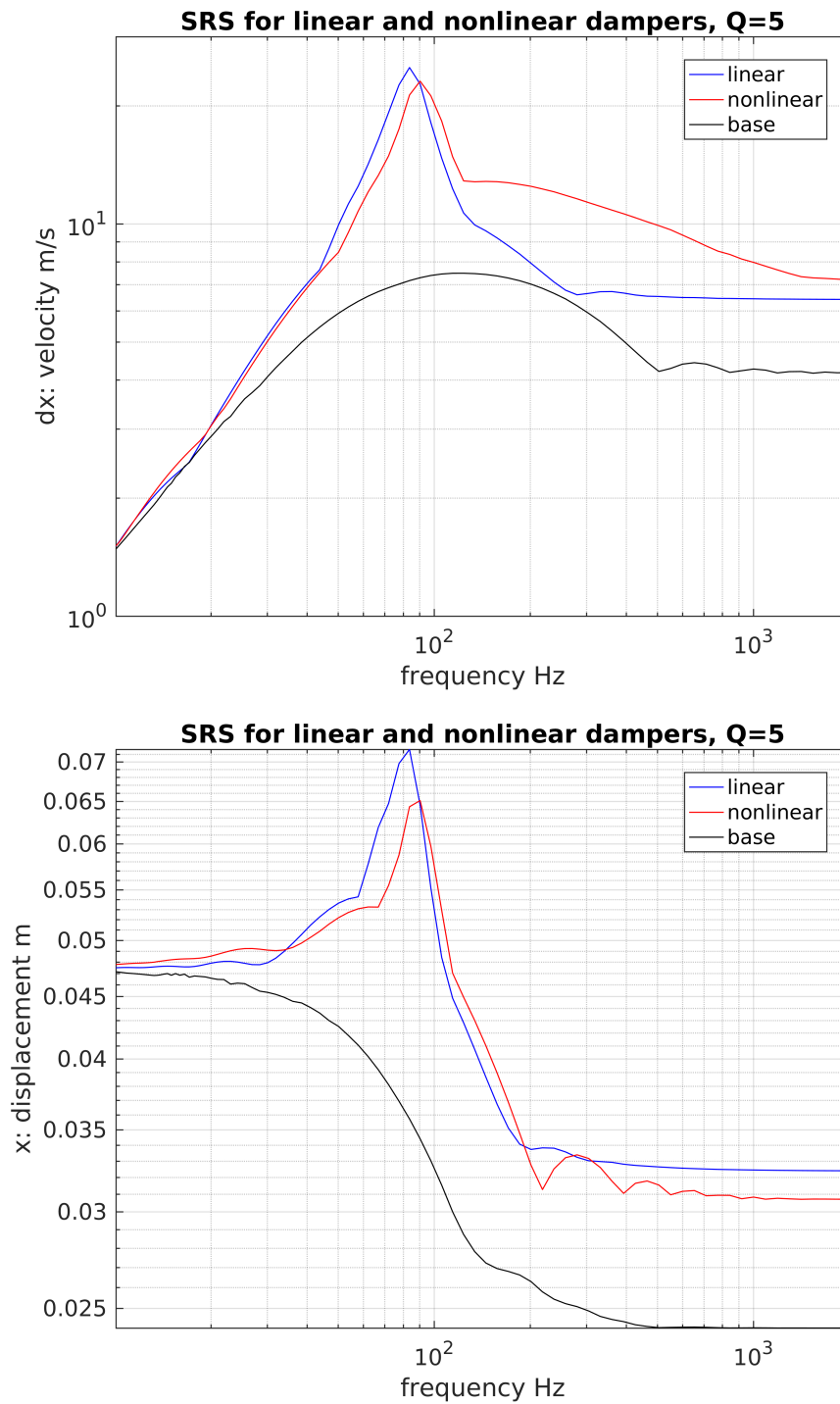


Figure 5.6 The upper plot shows the SRS for linear, nonlinear dampers and the base calculated from velocity \dot{x} . The lower plot shown the SRS based on displacement x .

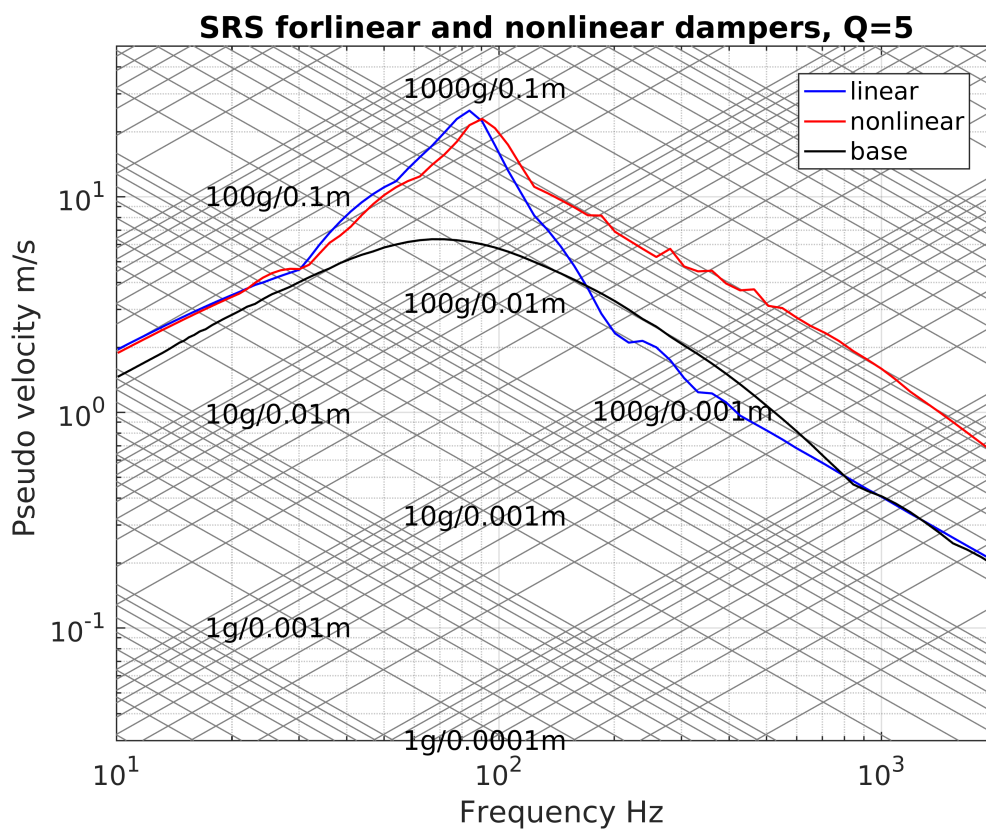


Figure 5.7 The plot shows a “tripartite” plot of the SRS for linear and nonlinear dampers. In tripartite plots pseudo velocity $v(f) = a(f)/(2\pi f)$ is plotted. Compared with the previous plots, where SRS are calculated based on velocity and displacement there are rather large deviations. That happens even for the linear case!

6 The Frahm damper and its effect on SRS

Consider a parallel damper model. Add to it a probe oscillator and a Frahm damper mass as shown in figure (6.1). The simulations show that the Frahm damper element when added to the main damper, enhances the damping. The Frahm damper has shown to be an efficient damper when the oscillations are harmonic. This is not obvious when it comes to shocks which are not harmonic.

Simulations here show that in fact the Frahm damper will have some effect on shock damping. The extra mass m_d will be able to absorb energy from the shock. Obviously more efficient with increasing mass and dissipation. Some results are shown in figure 6.2. Evidently as long as the frequency ω_d is close to the frequency ω , the damper is most efficient. The black curves show the SRS for the damper without the Frahm damper element. The other curves show the results when the Frahm damper is turned on. For $Q_d = 2.5$, there is damping at nearly all frequencies. At $Q_d = 10$, the damping occurs except in the parts of wings of the of the resonance frequency, where some amplification may occur. The latter is a known effect of the Frahm damper when applied to harmonic oscillations.

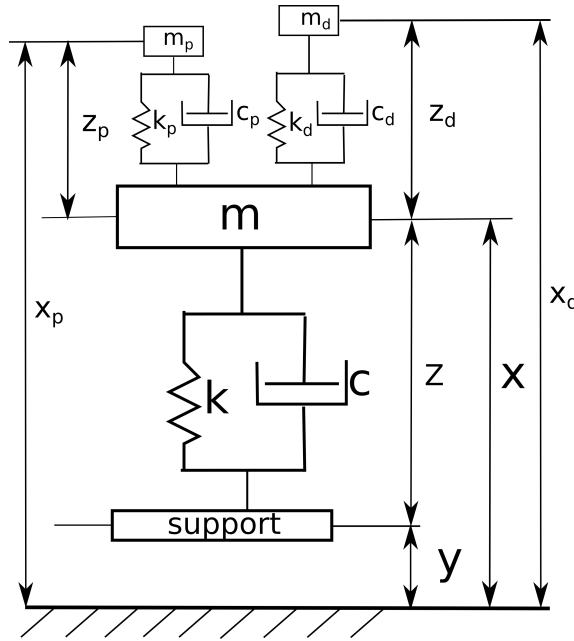


Figure 6.1 The parallel damper model with a SRS probe and a Frahm damper element

Let $x_p = x + z_p = y + z + z_p$, $x_d = x + z_d = y + z + z_d$ and $\omega^2 = k/m$, $\omega_p^2 = k_p/m_p$, $\omega_d^2 = k_d/m_d$, $\mu_p = m_p/m$, $\mu_d = m_d/m$, $2\zeta\omega = c/m$, $2\zeta_p\omega_p = c_p/m_p$, $2\zeta_d\omega_d = c_d/m_d$. The equations below are derived for arbitrary masses, stiffness and dissipation, but when $0 < m_p \ll 1$ it is used as a probe. The tunable mass is m_d . Finally

$$m_p \ddot{x}_p = -k_p z_p - c_p \dot{z}_p, \quad (6.1)$$

$$m_d \ddot{x}_d = -k_d z_d - c_d \dot{z}_d, \quad (6.2)$$

$$m \ddot{x} = -kz - c\dot{z} + k_p z_p + c_p \dot{z}_p + k_d z_d + c_d \dot{z}_d, \quad (6.3)$$

implying

$$\ddot{z} + 2\zeta\omega\dot{z} + \omega^2 z = \omega_p^2 \mu_p z_p + 2\zeta_p \omega_p \mu_p \dot{z}_p + \omega_d^2 \mu_d z_d + 2\zeta_d \omega_d \mu_d \dot{z}_d, \quad (6.4)$$

$$\ddot{z}_p + 2\zeta_p \omega_p (1 + \mu_p) + \omega_p^2 z_p = \omega^2 z + 2\zeta\omega\dot{z} - \omega_d^2 \mu_d z_d - 2\zeta_d \omega_d \mu_d \dot{z}_d, \quad (6.5)$$

$$\ddot{z}_d + 2\zeta_d \omega_d (1 + \mu_d) + \omega_d^2 z_d = \omega^2 z + 2\zeta\omega\dot{z} - \omega_p^2 \mu_p z_p - 2\zeta_p \omega_p \mu_p \dot{z}_p. \quad (6.6)$$

The accelerations are

$$\ddot{x} = -\omega^2 z - 2\zeta\omega\dot{z} + \omega_p^2 z_p + 2\zeta_p \omega_p \dot{z}_p + \omega_d^2 z_d + 2\zeta_d \omega_d \dot{z}_d,$$

$$\ddot{x}_p = -\omega_p^2 z_p - 2\zeta_p \omega_p \dot{z}_p,$$

$$\ddot{x}_d = -\omega_d^2 z_d - 2\zeta_d \omega_d \dot{z}_d.$$

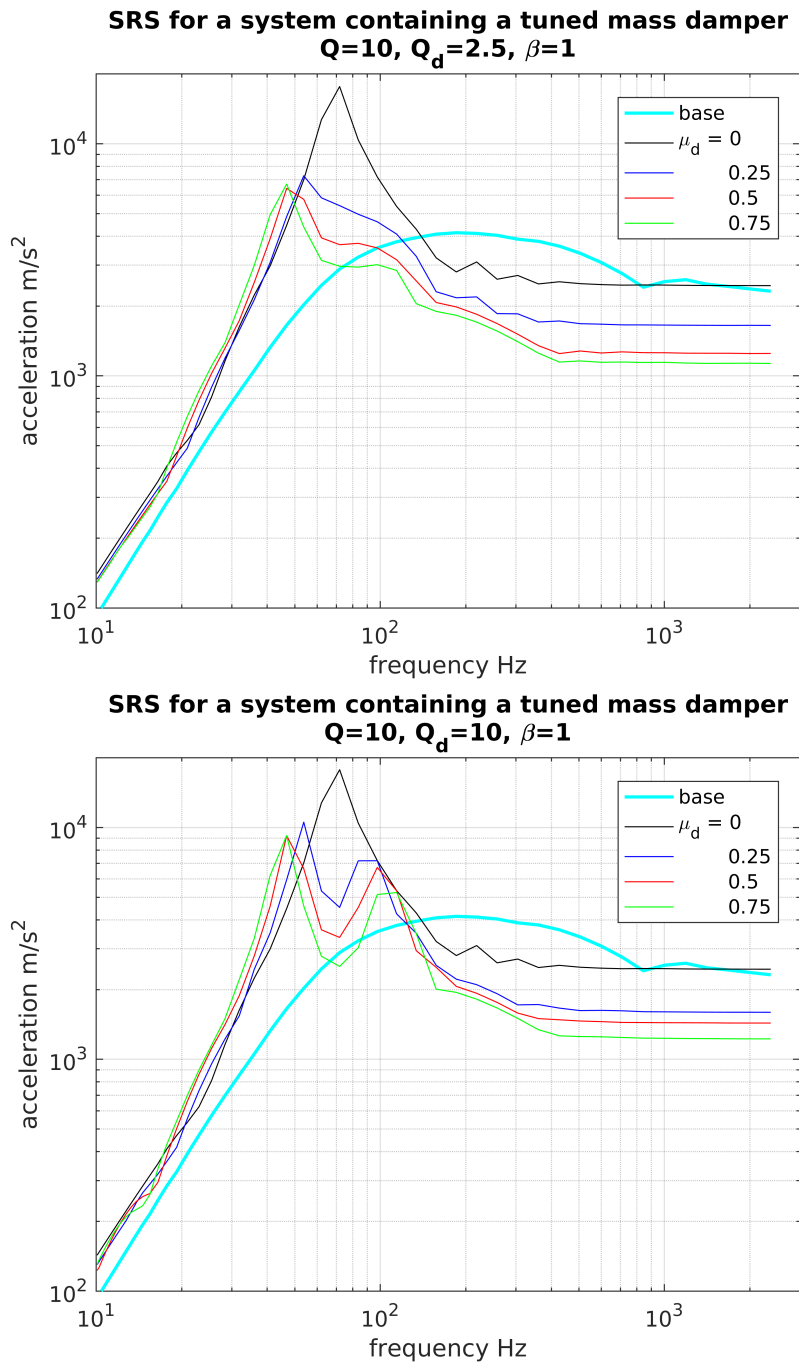


Figure 6.2 The left plot shows the SRS for a system based on a parallel damper with $Q = 10$ and with a tuned mass damper attached for selected mass fractions μ_d and $Q_d = 10$. The right panel shows the same but with $Q_d = 2.5$. The frequency of the Frahm damper is $\omega_d = \omega$

7 Conclusion

The motivation for this report was to study damper models, in particular models for rubber dampers and their impact to shock response. Dampers play an important role in military equipment by reducing the potentially devastating impacts of vibration and shock. The study was initiated by the need to characterize rubber dampers used in naval vessels. Characterization of dampers requires a good understanding on how dampers behave in relation to shock response and vibrations which was the motivation for this work. The knowledge obtained in this report will be used in a proceeding study which involves physical testing of dampers.

The simulation models developed here, permit exploration of case where Q , the stiffness k_1 and k_2 can vary. In the first cases, Q is varied, but assuming $k = k_1 = k_2$. Differences in results for the *parallel*, *combined* and the *standard* models are small in this case. The *serial* damper offers better damping in the sense of less acceleration (which requires more retarding space), but is of limited use due to its incapability to handle static loads.

In the next case studied, $Q = 5$, $k = k_1$ with fixed k_1 , while k_2 is varied. It appears that damping is sensitive to variation in k_2 . This can be used to construct damping systems that perform better compared with the parallel damping model. For rubber dampers it is plausible to assume that $k_1 \approx k_2$. This has to be explored further.

As shock is a violent process for which nonlinear models may describe the dynamics better than linear models. The study of nonlinearity is described through compression dependent stiffness. The result is striking where the SRS shows enhanced acceleration in the entire frequency band above the point where the SRS peaks. This has a most devastating effect on equipment. The bad accelerations are an effect of the damper being “saturated” as it is heavily compressed. When designing shock damper systems, care should be taken due to this effect. If possible by extended room for compression.

Finally, the Frahm damper and its effect on shock is studied. By adding an extra mass, the impact of the shock can be reduced by a factor of two. Additional mass is not a good idea if it is of no use, but perhaps there are situations where systems can be coupled together in such a way that the added mass has a purpose other than just being dead mass.

Further work:

This work has posed some new questions. It was necessary to limit parameter space to $k = k_1 = k_2$ and a few cases where $k_1 \neq k_2$. This should be explored further which is straightforward with the software developed here. The models can also be applied to other dampers than rubber dampers.

Pseudo-velocity and pseudo-displacement are quantities that are used in classical shock analysis and have defined a standard. This is mainly due to the fact that before mems-accelerometers were developed, velocity was measured in shock tests. The results were plotted on tripartite log paper, giving in addition “some picture” of displacement and acceleration. From shock simulations, both velocity and displacement are available and a study to compare calculated SRS-velocity and SRS-displacement should be compared with pseudo velocity and pseudo displacement derived from acceleration. Both linear and nonlinear cases should be studied.

The software developed here is structured such that any nonlinear stiffness-profile or any form of shock-profile can be implemented. For example it should be easy to implement random vibrations instead of the double half-sine functions used here.

A Matlab form of the damper equations

A.1 Parallel damper model

Matlab implementation. Parallel support system.
Equation (2.2) is written as two first order equations

$$\dot{z} = \xi, \quad (\text{A.1})$$

$$\dot{\xi} = -2\zeta\omega_n\xi - \omega_n^2z - \ddot{y}. \quad (\text{A.2})$$

Here $z = z(1)$, $\dot{z} = \xi = z(2)$.

The matlab form of equation (2.2) with the initial conditions. For harmonic excitation $y = \sin \omega t$, $\dot{y} = \omega \cos \omega t$, $\ddot{y} = -\omega^2 \sin \omega t$.

$$\text{Initial condition } z(1) = 0, z(2) = -\omega \Rightarrow \ddot{x}(0) = 2\zeta\omega_n\omega.$$

Governing equations general \ddot{y}

$$dz(1) = z(2),$$

$$dz(2) = -2\zeta\omega_nz(2) - \omega_n^2z(1) - \ddot{y}.$$

Acceleration

$$\ddot{x} = -2\zeta\omega_nz(2) - \omega_n^2z(1).$$

Initial conditions for pulse excitation

$$z(1) = 0, z(2) = 0 \Rightarrow \ddot{x}(0) = 0.$$

A.2 Serial damper model

Matlab implementation. Serial support system equations:

$$m\ddot{x} = -kz_b = -c\dot{z}_a.$$

Harmonic excitation $y = \sin \omega t$, $\dot{y} = \omega \cos \omega t$, $\ddot{y} = -\omega^2 \sin \omega t$.

The first order equations for the serial damper

$$\dot{z} = \xi, \quad (\text{A.3})$$

$$\dot{\xi} = -2\eta\omega_n\xi - \omega_n^2z - 2\eta\omega_n\dot{y} - \ddot{y}. \quad (\text{A.4})$$

Matlab form, governing equations

$$dz(1) = z(2),$$

$$dz(2) = -2\eta\omega_nz(2) - \omega_n^2z(1) - 2\eta\omega_n\dot{y} - \ddot{y}.$$

For the harmonic excitation the initial conditions are

$$z(1) = 0, z(2) = -\omega, \dot{x}(0) = 0, \Rightarrow \ddot{x}(0) = -2\eta\omega_n(\dot{y} + z(2)) - \omega_n^2z(1) = 0.$$

An equivalent way to solve the serial system is to write the governing equations in the form

$$\dot{z}_a = 2\eta\omega_n z_b, \quad (\text{A.5})$$

$$\dot{z}_b = \xi, \quad (\text{A.6})$$

$$\dot{\xi} = -2\eta\omega_n \xi - \omega_n^2 z_b - \ddot{y}. \quad (\text{A.7})$$

The matlab form is then

$$dz(1) = 2\eta\omega_n z(2),$$

$$dz(2) = z(3),$$

$$dz(3) = -2\eta\omega_n z(3) - \omega_n^2 z(2) - \ddot{y}.$$

The acceleration becomes simply for this system

$$m\ddot{x} = -kz_b \Rightarrow \ddot{x} = -\omega_n^2 z(2).$$

A.3 Combined damper model

The governing equations for the combined model can be written as follows

$$\dot{z}_a = 2\eta\omega_1 z_b,$$

$$\dot{z}_b = \xi,$$

$$\dot{\xi} = -2\eta\omega_1 \xi - (\omega_1^2 + \omega_2^2)z_b - \omega_2^2 z_a - \ddot{y}.$$

Using the harmonic forcing $y = \sin \omega t$ the initial conditions are $(z_a, z_b, \dot{z}_b) = (0, 0, -\omega)$, where $z_a = z(1)$, $z_b = z(2)$, $\dot{z}_b = \xi = z(3)$.

$$dz(1) = 2\eta\omega_1 z(2),$$

$$dz(2) = z(3),$$

$$dz(3) = -2\eta\omega_1 z(3) - (\omega_1^2 + \omega_2^2)z(2) - \omega_2^2 z(1) - \ddot{y}.$$

For diagnostic purposes

$$x = z(1) + z(2) + y,$$

$$\dot{x} = 2\eta\omega_1 z(2) + z(3) + \dot{y},$$

$$\ddot{x} = -\omega_2^2 z(1) - (\omega_1^2 + \omega_2^2)z(2),$$

implying $(x(0), \dot{x}(0), \ddot{x}(0)) = (0, 0, 0)$ for the harmonic excitation.

For the double half-sine pulse, also $\dot{z}_b(0) = 0$.

A.4 Standard damper model

Equations (2.12) and (2.13) can be written as a first order system

$$\dot{z}_a = 2\eta_1\omega_1 \left(z_b - (\omega_2/\omega_1)^2 z_a \right), \quad (\text{A.8})$$

$$\dot{z}_b = \xi, \quad (\text{A.9})$$

$$\dot{\xi} = -2\eta_1\omega_1 \xi - \omega_1^2 (1 - (2\eta_1\omega_2/\omega_1)^2) z_b - \omega_2^2 (2\eta_1\omega_2/\omega_1)^2 z_a - \ddot{y}. \quad (\text{A.10})$$

Matlab implementation

$$dz(1) = 2\eta_1\omega_1 \left(z(2) - (\omega_2/\omega_1)^2 z(1) \right),$$

$$dz(2) = z(3),$$

$$dz(3) = -2\eta_1\omega_1 z(3) - \omega_1^2 (1 - (2\eta_1\omega_2/\omega_1)^2) z(2) - \omega_2^2 (2\eta_1\omega_2/\omega_1)^2 z(1) - \ddot{y}$$

Diagnostics

$$x = z(1) + z(2) + y,$$

$$\dot{x} = 2\eta_1\omega_1 \left(z(2) - (\omega_2/\omega_1)^2 z(1) \right) + z(3) + \dot{y},$$

$$\ddot{x} = -\omega_1^2 z(2).$$

B Equations for SRS of dampers on matlab form

B.1 SRS model for parallel damper

Equation for SRS for parallel damper written on first order form

$$\begin{aligned}\dot{z} &= \xi, \\ \dot{\xi} &= -2\zeta\omega\xi - \omega^2z + 2\zeta_p\omega_p\mu\psi + \omega_p^2\mu z_p - \ddot{y}, \\ \dot{z}_p &= \psi, \\ \dot{\psi} &= -2\zeta_p\omega_p(1 + \mu)\psi - \omega_p^2(1 + \mu)z_p + 2\zeta\omega\xi + \omega^2z.\end{aligned}$$

Matlab implementation

$$\begin{aligned}z(1) &= z, & dz(1) &= z(2), \\ z(2) &= \xi = \dot{z}, & dz(2) &= -2\zeta\omega z(2) - \omega^2z(1) + 2\zeta_p\omega_p\mu z(4) + \omega_p^2\mu z(3) - \ddot{y}, \\ z(3) &= z_p, & dz(3) &= z(4), \\ z(4) &= \psi = \dot{z}_p. & dz(4) &= -2\zeta_p\omega_p(1 + \mu)z(4) - \omega_p^2(1 + \mu)z(3) + 2\zeta\omega z(2) + \omega^2z(1).\end{aligned}$$

Accelerations

$$\begin{aligned}\ddot{x}_p &= -2\zeta_p\omega_p z(4) - \omega_p^2 z(3), \\ \ddot{x} &= -2\zeta\omega z(2) - \omega^2 z(1) + 2\zeta_p\omega_p\mu z(4) + \omega_p^2\mu z(3).\end{aligned}$$

B.2 SRS model for serial damper

SRS model for the serial damper on first order form

$$\dot{z}_a = 2\eta\omega z_b, \tag{B.1}$$

$$\dot{z}_b = \xi, \tag{B.2}$$

$$\dot{\xi} = -2\eta\omega\xi - \omega^2z_b + 2\zeta_p\omega_p\mu\psi + \omega_p^2\mu z_p - \ddot{y}, \tag{B.3}$$

$$\dot{z}_p = \psi, \tag{B.4}$$

$$\dot{\psi} = -2\zeta_p\omega_p(1 + \mu)\psi - \omega_p^2(1 + \mu)z_p + \omega^2z_b. \tag{B.5}$$

Matlab implementation

$$\begin{aligned}z(1) &= z_a, & dz(1) &= 2\eta\omega z(2), \\ z(2) &= z_b, & dz(2) &= z(3), \\ z(3) &= \dot{z}_b = \xi, & dz(3) &= -2\eta\omega z(3) - \omega^2z(2) + 2\zeta_p\omega_p\mu z(5) + \omega_p^2\mu z(4) - \ddot{y}, \\ z(4) &= z_p, & dz(4) &= z(5), \\ z(5) &= \dot{z}_p = \psi. & dz(5) &= -2\zeta_p\omega_p(1 + \mu)z(5) - \omega_p^2(1 + \mu)z(4) + \omega^2z(2).\end{aligned}$$

Accelerations

$$\begin{aligned}\ddot{x} &= -\omega^2 z(2) + 2\zeta_p \omega_p \mu z(5) + \omega_p^2 \mu z(4), \\ \ddot{x}_p &= -2\zeta_p \omega_p z(5) - \omega_p^2 z(4).\end{aligned}$$

B.3 SRS model for the combined damper

The equations for the SRS model for the combined damper are

$$\begin{aligned}\dot{z}_a &= 2\eta\omega_1 z_b, \\ \dot{z}_b &= \xi, \\ \dot{\xi} &= -2\eta\omega_1 \xi - (\omega_1^2 + \omega_2^2)z_b - \omega_2^2 z_a + 2\zeta_p \omega_p \mu \psi + \omega_p^2 \mu z_p - \ddot{y}, \\ \dot{z}_p &= \psi, \\ \dot{\psi} &= -2\zeta_p \omega_p (1 + \mu)\psi - \omega_p^2 (1 + \mu)z_p + \omega_2^2 z_a + (\omega_1^2 + \omega_2^2)z_b.\end{aligned}$$

Matlab implementation

$$\begin{aligned}z(1) &= z_a, & dz(1) &= 2\eta\omega_1 z(2), \\ z(2) &= z_b, & dz(2) &= z(3), \\ z(3) &= \dot{z}_b = \xi, & dz(3) &= -2\eta\omega_1 z(3) - (\omega_1^2 + \omega_2^2)z(2) - \omega_2^2 z(1) + 2\zeta_p \omega_p \mu z(5) + \omega_p^2 \mu z(4) - \ddot{y}, \\ z(4) &= z_p, & dz(4) &= z(5), \\ z(5) &= \dot{z}_p = \psi. & dz(5) &= -2\zeta_p \omega_p (1 + \mu)z(5) - \omega_p^2 (1 + \mu)z(4) + \omega_2^2 z(1) + (\omega_1^2 + \omega_2^2)z(2).\end{aligned}$$

Accelerations

$$\begin{aligned}\ddot{x}_p &= -\omega_p^2 z(4) - 2\zeta_p \omega_p z(5), \\ \ddot{x} &= -\omega_2^2 z(1) - (\omega_1^2 + \omega_2^2)z(2) + \omega_p^2 \mu z(4) + 2\zeta_p \omega_p \mu z(5).\end{aligned}$$

B.4 SRS model for the standard damper

First order form of the equations for the SRS model for the standard damper

$$\begin{aligned}\dot{z}_a &= 2\eta_1 \omega_1 \left(z_b - (\omega_2/\omega_1)^2 z_a \right), \\ \dot{z}_b &= \xi, \\ \dot{\xi} &= -2\eta_1 \omega_1 \xi - \omega_1^2 \left(1 - (2\eta_1 \omega_2/\omega_1)^2 \right) z_b - \omega_2^2 (2\eta_1 \omega_2/\omega_1)^2 z_a + \omega_p^2 \mu z_p + 2\zeta_p \omega_p \mu \psi - \ddot{y}, \\ \dot{z}_p &= \psi, \\ \dot{\psi} &= -2\zeta_p \omega_p (1 + \mu)\psi - \omega_p^2 (1 + \mu)z_p + \omega_1^2 z_b.\end{aligned}$$

Matlab implementation

$$\begin{aligned}
dz(1) &= 2\eta_1\omega_1\left(z(2) - (\omega_2/\omega_1)^2z(1)\right), \\
z(1) = z_a, \quad dz(2) &= z(3), \\
z(2) = z_b, \quad dz(3) &= -2\eta_1\omega_1z(3) - \omega_1^2\left(1 - (2\eta_1\omega_2/\omega_1)^2\right)z(2) - \omega_2^2(2\eta_1\omega_2/\omega_1)^2z(1) \\
z(3) = \dot{z}_b = \xi, \quad &+ \omega_p^2\mu z(4) + 2\zeta_p\omega_p\mu z(5) - \ddot{y}, \\
z(4) = z_p, \quad dz(4) &= z(5), \\
z(5) = \dot{z}_p = \psi. \quad dz(5) &= -2\zeta_p\omega_p(1 + \mu)z(5) - \omega_p^2(1 + \mu)z(4) + \omega_1^2z(2).
\end{aligned}$$

Accelerations

$$\begin{aligned}
\ddot{x}_p &= -\omega_p^2z(4) - 2\zeta_p\omega_pz(5), \\
\ddot{x} &= -\omega_1^2z(2) + \omega_p^2\mu z(4) + 2\zeta_p\omega_p\mu z(5).
\end{aligned}$$

B.5 Matlab implementation, Frahm damper

For matlab implementation

$$\begin{pmatrix} z(1) \\ z(2) \\ z(3) \\ z(4) \\ z(5) \\ z(6) \end{pmatrix} = \begin{pmatrix} z \\ \dot{z} \\ z_p \\ \dot{z}_p \\ z_d \\ \dot{z}_d \end{pmatrix}.$$

C Matlab code for calculating SRS for the parallel damper, example parallel damper

This implementation use the equations presented in appendix (B.1).

```

1 function SRSparams ()
2 global SRSdhs % defines the double half-sine
3 SRSdhs.A = 2250; % acceleration m/s^2
4 SRSdhs.t1 = 0.0029; % duration first half-pulse
5 SRSdhs.t2 = 0.0116; % duration second half-pulse
6
7 global SRSprobe % data for SRS probe
8 SRSprobe.Q = 50; % Q factor
9 SRSprobe.mu = 0.0001; % mu = m_p/m
10
11 global phys % definitions in physical space (time domaine)
12 phys.m = 12; % duration factor for integration T=m*(t1+t2)
13 phys.n = 15; % number of damper oscillations within [0,T]
14 % phys.m = 24; % duration factor for integration T=m*(t1+t2)
15 % phys.n = 8; % number of damper oscillations within [0,T]
16 phys.npts = 1600; % number of points in time domaine
17
18 global spec % definition of points in spectral space
19 spec.nf = 120; % number of frequency points
20 spec.f0 = 2^(1/8); % separation between frequency points
21 spec.fak = 0.036*2; % scale factor for frequency data
22 spec.fstart = 10; % lowest frequency in spectrum

1 function SRsrapport(Q)
2 % calculating SRS for DOUBLE HLAIF SINE shock, parallel damper
3 % use: SRsrapport(Q)
4 % input: Q quality factor for oscillator m
5 % parameters see SRSparams.m
6
7 SRSparams() % defines parameters
8
9 global SRSdhs
10 A = SRSdhs.A;
11 t1 = SRSdhs.t1;
12 t2 = SRSdhs.t2;
13
14 global SRSprobe
15 Qp = SRSprobe.Q;
16 mu = SRSprobe.mu;
17
18 global phys
19 m = phys.m;
20 n = phys.n;
21 npts = phys.npts;
22
23 global spec
24 nf = spec.nf;
25 f0 = spec.f0;
26 fak = spec.fak;
27 fstart = spec.fstart;
28
29
30 T = m*(t1+t2); % duration for shock calculation
31 omega = 2*pi*n/T; % circular frequency damper oscillator
32 zeta = 1/(2*Q); % damping parameter damper oscillator
33 zetap = 1/(2*Qp); % damping parameter probe oscillator
34 % initial conditions
35 Z10 = 0; dZ10 = 0; Z20 = 0; dZ20 = 0;
36 Zinit = [Z10,dZ10,Z20,dZ20];
37 %
38 tspan = linspace(0.0,T,npts); % points in time frame
39
40 acc = @myacc; % dhs acceleration
41 vel = @myvel;
42 dis = @mydisp;
43
44 a = zeros(npts,1); % array containing support acceleration
45 ve = zeros(npts,1); % array containing support velocity
46 di = zeros(npts,1); % array containing support displacement
47
48 ddx2 = zeros(npts,nf); % array containing accelerations for probes
49 ff = zeros(nf,1); % array containing frequency points
50 ddx2max = zeros(nf,1); % array containing SRS data
51 disp(['SRS calculated for parallel damper: Q=' ,...
52 num2str(Q) , ', f=' , num2str(omega/(2*pi)) , 'Hz, nf=' , int2str(nf)])
53 %
54 to = 1;
55 for i=1:nf
56 to = f0*to;
57 ff(i) = fak*to + fstart;

```

```

58     frek = fak*to + fstart;
59     omegap = 2*pi*frek; % probe frequency
60 %solver using RK45 solution arrays at tspan
61 % z(:,1)=z, z(:,2)=dz, z(:,3) = z_p, z(:,4) = dz_p
62 [t,z]=ode45(@(t,z) ddSRSpar(t,z,zeta,zetap,omega,omegap,mu,...
63             acc),tspan,Zinit);
64     ddx2(:,i) = -omegap^2*z(:,3) - 2*zetap*omegap*z(:,4); % probe solutions
65     ddx2max(i) = max(abs(ddx2(:,i))); % SRS based on max(abs)
66 end
67 % taken out of loop since mu << 1, ddx1 not dependent on m_p motion
68 ddx1 = -omega^2*z(:,1) - 2*zeta*omega*z(:,2) + omegap^2*mu*z(:,3) + ...
69       2*zetap*omegap*mu*z(:,4); % acceleration of m
70
71 for i = 1:npts
72     a(i) = acc(tspan(i)); % acceleration of support
73     ve(i) = vel(tspan(i)); % velocity
74     di(i) = dis(tspan(i)); % displacement
75 end
76
77 fig = 1; % plot of DHS, damper oscillations and probes
78 figure(fig)
79 clf(fig)
80 p(1) = plot(t,a,'g','LineWidth',1.5);
81 hold on
82 p(2) = plot(t,ddx1,'r','LineWidth',1.5);
83 for i=1:nf
84     plot(t,ddx2(:,i))
85 end
86 xlabel('time s')
87 ylabel('acceleration m/s^2')
88 title(['Parallel damper Q=',num2str(Q),'']);
89 legend([p(1),p(2)],'Support acceleration','Damper response')
90 grid on
91
92 fig = fig + 1; % plot of SRS
93 figure(fig)
94 clf(fig)
95 loglog(ff,ddx2max,'b')
96 hold on
97 [fb,ddxbase] = MSRSbase();
98 loglog(fb,ddxbase,'k')
99 grid on
100 xlim([ff(1) ff(nf)])
101 ylim([min(ddx2max) max(ddx2max)])
102 xlabel('frequency Hz')
103 ylabel('acceleration m/s^2')
104 legend('m','base')
105 title(['SRS for parallel damper Q=',num2str(Q)])

```

Solvers, functions for acceleration, velocity and displacement for a double half-sine pulse, see chapter (3).

```

1 function [ff,ddxmax] = MSRSbase()
2 % calculating SRS for the base moving as DOUBLE HALF SINE shock,
3 % see definitions in file SRSparams.m
4 %
5 % use: [ff,ddxmax] = SRSbase()
6 % input: parameters defined in SRSparams.m
7 % output:
8 %     ff      frequency data
9 %     ddxmax  SRS data
10 %
11 global SRSdhs
12 A = SRSdhs.A;
13 t1 = SRSdhs.t1;
14 t2 = SRSdhs.t2;
15
16 global phys
17 m = phys.m;
18 n = phys.n;
19 npts = phys.npts;
20
21 global SRSprobe
22 Qp = SRSprobe.Q;
23 mu = SRSprobe.mu;
24
25 global spec
26 nf = spec.nf;
27 f0 = spec.f0;
28 fak = spec.fak;
29 fstart = spec.fstart;
30
31
32 if t1 > t2
33     disp('Error t2 > t1')
34     ff=0;ddxmax=0;
35     return
36 end

```

```

37 disp(['Computing SRS for base Qp=',num2str(Qp)])
38 T = m*(t1+t2); % time duration for shock calculation
39 zeta = 1/(2*Qp);
40 Z = 0;
41 dZ= 0;
42 Zinit = [Z,dZ];
43
44 tspan = linspace(0.0,T,npts);
45
46 acc = @myacc;
47 %
48 % SRS calculation
49 %
50 ff = zeros(nf,1);
51 ddxmax = zeros(nf,1);
52 disp(['Base: zeta=',num2str(zeta),' , numpts =',int2str(nf)])
53
54 to = 1;
55 for i=1:nf
56     to = f0*to;
57     ff(i) = fak*to + fstart;
58     frek = fak*to + fstart;
59     omi = 2*pi*frek;
60     [t,z] = ode45(@(t,z) ddMBase(t,z,zeta,omi,acc), tspan, ...
61                 Zinit);
62     ddx = -2*zeta*omi*z(:,2) - omi^2*z(:,1); % probe acceleration
63     ddxmax(i) = max(abs(ddx));
64 end

1 function dz = ddMBase(t,z,zeta,om,acc)
2 % solving support system parallel oscillator
3 % for specified acc, for example double half sine shock
4 %
5 dz = zeros(2,1);
6 dz(1) = z(2);
7 dz(2) = -2*zeta*om*z(2) - om^2*z(1) - acc(t);

1 function dz = ddSRSpars(t,z,zeta,zetap,omega,omegap,mu,acc)
2 % solver for a PARALLEL (spring, dashpot) support system excited by a
3 % pulse defined by function acc.
4 % Damping parameter is zeta=1/(2Q) and frequency is omega.
5 % The probe mass mp has damping parameter zetap and frequency omegap.
6 % The script is general, not dependent on the mass fraction mu=mp/m.
7 % When mp is used as an SRS probe, set m >0 and m << 1.
8 % The double half sine pulse is defined by t1, t2 and A as
9 % set in SRSParams.m
10 dz = zeros(4,1);
11 dz(1) = z(2);
12 dz(2) = -2*zeta*omegap*z(2) - omegap^2*z(1) +2*zetap*omegap*mu*z(4) ...
13     + omegap^2*mu*z(3) - acc(t);
14 dz(3) = z(4);
15 dz(4) = -2*zetap*omegap*(1+mu)*z(4) - omegap^2*(1+mu)*z(3) ...
16     + 2*zeta*omegap*z(2) + omegap^2*z(1);

1 function acc = myacc(t)
2 % double half sine (dhs) acceleration for SRS calculations
3 % t instant for which acceleration is to be calculated
4 % t1 duration first part of dhs
5 % t2 duration of second part of dhs
6 % A amplitude m/s^2
7 % acc = @myacc
8 % a = acc(t), acceleration calculated at time t
9 global SRSDhs
10 A = SRSDhs.A;
11 t1 = SRSDhs.t1;
12 t2 = SRSDhs.t2;
13
14 if (0 <= t) && (t <= t1)
15     acc = A*sin((pi/t1)*t);
16 elseif (t1 < t) && (t <= t2)
17     acc = -A*(t1/(t2-t1))*sin(pi*(t-t1)/(t2-t1));
18 else
19     acc = 0;
20 end

1 function vel = myvel(t)
2 % double half sine (dhs) velocity for SRS caclulations
3 % corresponding to quantities defined in acceleration.m
4 % t instant for which acceleration is to be calculated
5 % t1 duration first part of dhs
6 % t2 duration of second part of dhs
7 % A amplitude m/s^2 defined in acceleration.m
8 % vel = @myvel
9 % v = vel(t) % velocity calculated at time t
10 global SRSDhs
11 A =SRSDhs.A;
12 t1=SRSDhs.t1;

```

```

13  t2=SRSdhs.t2;
14
15  K = A*(t1/pi);
16  if (0 <= t) && (t <= t1)
17      vel = K*(1-cos((pi/t1)*t));
18  elseif (t1 < t) && (t <= t2)
19      vel = K*(1+cos((pi*(t-t1)/(t2-t1))));
20  else
21      vel=0;
22  end

1  function dis = mydisp(t)
2  % double half sine (dhs) displacement for SRS calculations
3  % corresponding to quantities defined in acceleration.m
4  % t      instant for which acceleration is to be calculated
5  % t1     duration first part of dhs
6  % t2     duration of second part of dhs
7  % A      amplitude m/s^2 defined in acceleration.m
8  % dis = @mydisp
9  % d = dis(t) displacement calculated at time t;
10 global SRSdhs
11 A = SRSdhs.A;
12 t1= SRSdhs.t1;
13 t2= SRSdhs.t2;
14
15 K = A*(t1/pi);
16 if (0 <= t) && (t <= t1)
17     dis = K*(t - (t1/pi)*sin((pi/t1)*t));
18 elseif (t1 < t) && (t <= t2)
19     dis = K*(t + ((t2-t1)/pi)*sin(pi*(t-t1)/(t2-t1)));
20 else
21     dis=K*t2;
22 end

```

References

- [1] Ø. Andreassen. Introduction to shock-response spectra. Technical report, Norwegian Defence Research Establishment (FFI), FFI-RAPPORT 20/1912, 2020.
- [2] J. J. M de Bever. Dynamic behaviour of rubber and rubberlike materials. Technical report, Eindhoven University of Technology, 1992. WFW-report:92.006.
- [3] Hermann Frahm. Us patent 989,957, 1909.
- [4] P Hagedorn and G Spelsberg-Korspeter, editors. *Active and Passive Vibration Control of Structures*, volume 558. Springer, 2014. ISBN-978-3-7091-1820-7.
- [5] J. P. Den Hartog. *Mechanical Vibrations*. Dover Publicaitons, inc, 1956.
- [6] D. W. Jordan and P. Smith. *Nonlinear Ordinary Differential Equations*. Number ISBN-0199208255 in 4th edition. Oxford, 2007.
- [7] D. C. K. Poon, Shaw.song Shieh, L. M. Joseph, and Ching-Chang Chang. Structural design of taipei 101, the worlds tallest building. In *CTBHU 2004 Seoul Conference*, pages 271–278, Seoul, Korea, October 2004. CTBHU. Concrete. Outriggers. Structure. Tuned Mass Damper.
- [8] W. T. Thomson and M. D. Dahleh. *Theory of Vibration with Applications*. Prentice Hall, Upper Saddle River, New Jersey 078458, 5'th ed edition, 1998. ISBN 0-13-651068-X.
- [9] *Hutchinson Industry catalog*. www.paulstra-industry.com.

About FFI

The Norwegian Defence Research Establishment (FFI) was founded 11th of April 1946. It is organised as an administrative agency subordinate to the Ministry of Defence.

FFI's mission

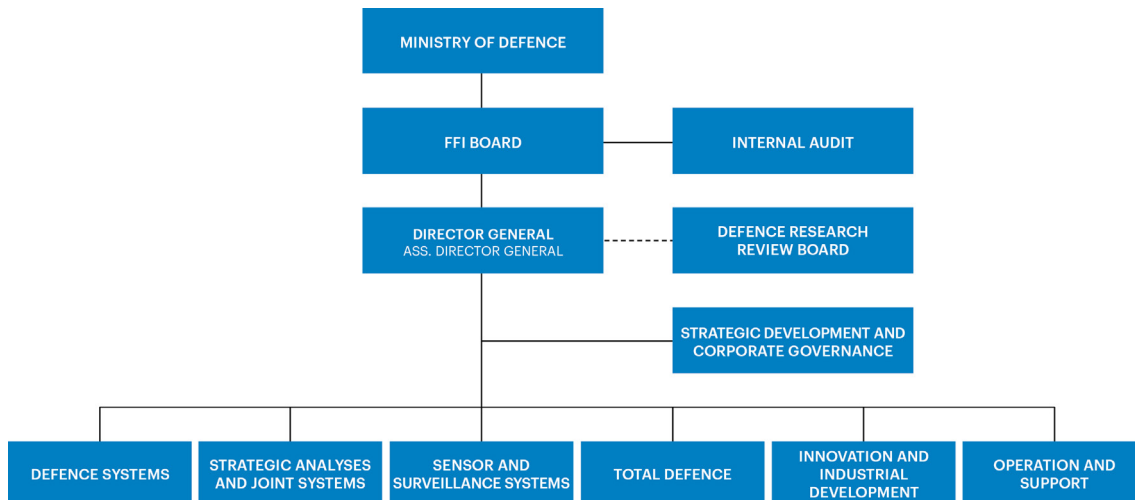
FFI is the prime institution responsible for defence related research in Norway. Its principal mission is to carry out research and development to meet the requirements of the Armed Forces. FFI has the role of chief adviser to the political and military leadership. In particular, the institute shall focus on aspects of the development in science and technology that can influence our security policy or defence planning.

FFI's vision

FFI turns knowledge and ideas into an efficient defence.

FFI's characteristics

Creative, daring, broad-minded and responsible.



Forsvarets forskningsinstitutt (FFI)
Postboks 25
2027 Kjeller

Besøksadresse:
Kjeller: Instituttveien 20, Kjeller
Horten: Nedre vei 16, Karljohansvern, Horten

Telefon: 91 50 30 03
E-post: post@ffi.no
ffi.no

Norwegian Defence Research Establishment (FFI)
PO box 25
NO-2027 Kjeller
NORWAY

Visitor address:
Kjeller: Instituttveien 20, Kjeller
Horten: Nedre vei 16, Karljohansvern, Horten

Telephone: +47 91 50 30 03
E-mail: post@ffi.no
ffi.no/en